INVESTIGATION OF SOME PHYSICAL PROPERTIES OF Ce-DOPED Bi–2212

by

YUSUF ZALAOĞLU

THESIS SUBMITTED TO

THE GRADUATE SCHOOL OF NATURAL AND APPLIED SCIENCES

OF

THE ABANT İZZET BAYSAL UNIVERSITY

IN PARTIAL FULFILLMENT OF THE REQUIREMENTS FOR THE DEGREE

OF

MASTER OF SCIENCE

IN

THE DEPARTMENT OF PHYSICS

JUNE 2011

Approval of the Graduate School of Natural and Applied Science

Prof. Dr. Nihat ÇELEBİ
Director

I certify that this thesis satisfies all the requirements as a thesis for the degree of Master of Science.

Prof. Dr. Kıvılcım KILIÇ
Head of Physics Department

This is to certify that we have read this thesis and that in our opinion it is fully adequate, in scope and quality as a thesis for the degree of Master of Science.

Prof. Dr. Ahmet VARİLCİ
Co-Supervisor

Assoc. Prof. Dr. Cabir TERZİOĞLU
Supervisor

Examining Committee Members:

1. Assoc. Prof. Dr. Cabir TERZİOĞLU …….
2. Assoc. Prof. Dr. Oğuz ÜSTÜN …….
3. Assist. Prof. Dr. Cihan PARLAK …….

ABSTRACT

INVESTIGATION OF SOME PHYSICAL PROPERTIES OF Ce-DOPED Bi–2212

ZALAOĞLU, Yusuf

M.S., Department of Physics

Supervisor: Assoc. Prof. Dr. Cabir TERZİOĞLU

Co-Supervisor: Prof. Dr. Ahmet VARİLCİ

June 2011, 73 Pages

In this study, the structural and superconducting properties of compounds prepared by doping Cerium to Bi–2212 system in the form of $Bi_2Sr_2Ca_1Cu_2Ce_xO_y$ (x=0, 0.001, 0.003, 0.005, 0.01, 0.03, 0.05, 0.1) were investigated. All samples were prepared using the standard solid-state reaction method. In order to make comparison with the pure sample (x=0), all samples were prepared under the same conditions. While the structural characterization of all samples were carried out with X–Ray Diffraction(XRD) and Scanning Electron Microscopy(SEM) measurements, electrical and superconducting properties of the samples were performed via resistivity measurements. Based on the results of resistivity measurements of the samples done in the case of magnetic field, as it was observed that the critical onset

temperature(T_c^{onset}) increased with increase in Cerium addition until 0.05 above which the onset point of the sample rapidly started to decrease. However, the critical offset temperature(T_c^{offset}) was found to decrease with increasing Cerium concentration and applied magnetic field. Besides, it was noticed that all samples showed metallic behaviour above T_c^{onset} temperature. Moreover, the resistivity (at room temperature) was also observed to increase with the increase in the addition of the Cerium atoms. As for XRD measurements, all lattice parameters and phases corresponding to peaks on X-ray diffraction graphs were determined by means of literature. Furthermore, volume fractions of Bi–2223 and Bi–2212 phases were calculated for all samples. It was clearly found that the fraction of Bi–2212 phase was greater than the fraction of Bi–2223 phase. However, the volume fraction of Bi–2223 phase increased up to an optimum concentration value(x=0.05). As it is well known the critical onset temperature(T_c^{onset}) of a sample increases with the increase in the Bi–2223 volume fraction. This situation was also observed at resistivity measurements. Therefore, we can clearly say that XRD measurements are found to be in good agreement with resistivity measurements. Moreover, surface morphology and grain connectivity of the samples were obtained to degrade with increase in the Cerium addition from SEM investigations. To sum up, Cerium addition was found to supress the superconducting properties.

KEYWORDS: High-temperature superconductors, Bi–2223, Bi–2212, Cerium, Critical Onset Temperature.

ÖZET

Ce-KATKILI Bi-2212'NİN BAZI FİZİKSEL ÖZELLİKLERİNİN İNCELENMESİ

ZALAOĞLU, Yusuf

Yüksek Lisans, Fizik Bölümü

Tez Danışmanı: Doç. Dr. Cabir TERZİOĞLU

Ortak Tez Danışmanı: Prof. Dr. Ahmet VARİLCİ

Haziran 2011, 73 Sayfa

Bu çalışmada, Bi–2212 sistemine $Bi_2Sr_2Ca_1Cu_2Ce_xO_y$ (x=0, 0.001, 0.003, 0.005, 0.01, 0.03, 0.05, 0.1) formunda Seryum katkılanarak hazırlanan bileşiklerin yapısal ve süperiletkenlik özellikleri incelendi. Tüm örnekler katıhal tepkime yöntemi kullanılarak hazırlandı. Saf numune ile karşılaştırma yapabilmek için tüm örnekler aynı koşullarda hazırlandı. Tüm örneklerin yapısal karakterizasyonu X-Işını Kırınımı(XRD) ve Taramalı Elektron Mikroskobu(SEM) yardımıyla gerçekleştirilirken elektrik ve süperiletkenlik özellikleri özdirenç ölçümleriyle belirlendi. Manyetik alan altında yapılan özdirenç ölçümlerinin sonuçlarına dayanılarak, süperiletkenlik başlangıç sıcaklığının hızla azalmaya başladığı 0.05'in üzerindeki değerlere kadar Seryum katkısının artmasıyla başlangıç sıcaklığının arttığı

gözlendi. Bununla birlikte süperiletkenlik bitiş sıcaklığında Seryum konsantrasyonunun ve uygulanan manyetik alanın artmasıyla azalma belirlendi. Ayrıca tüm numunelerin T_c^{onset} sıcaklığının üzerinde metalik özelliği gösterdiği saptandı. Dahası özdirencin(oda sıcaklığında) Seryum atomlarının katkılamasının artmasıyla arttığı gözlendi. XRD ölçümlerine gelince, X-ışını kırınımı grafiklerindeki piklere karşılık gelen tüm örgü parametreleri ve fazlar literatür yardımıyla belirlendi. Üstelik Bi–2223 ve Bi–2212 fazlarının hacim oranları tüm numuneler için hesaplandı. Bi–2212 faz oranının Bi–2223 faz oranından daha büyük olduğu açıkça bulundu. Halbuki Bi–2223 hacim oranı ideal konsantrasyon değerine(x=0.05) kadar arttı. Bilindiği gibi süperiletkenlik başlangıç sıcaklığı Bi–2223 hacim oranının artmasıyla artar. Bu durum özdirenç ölçümlerinde de gözlendi. Bu yüzden XRD ölçümlerinin özdirenç ölçümleriyle uyum içerisinde olduğu açıkça söylenebilir. Dahası SEM ölçümlerinden Seryum katkılamasının artmasıyla numunelerin yüzey biçiminin ve tanecik bağlantısının azaldığı belirlendi. Sonuç olarak, Seryum katkılamasının süperiletkenlik özellikleri kötüleştirdiği bulundu.

ANAHTAR KELİMELER: Yüksek-Sıcaklık Süperiletkenleri, Bi–2223, Bi–2212, Seryum, Kritik Başlangıç Sıcaklığı.

To My Parents…

ACKNOWLEDGEMENT

I would like to thank many people who have contributed to the completion of this thesis.

First of all, I would like to thank my supervisor Assoc. Prof. Dr. Cabir Terzioğlu for his guidance, valuable suggestions, encouragement and patience throughout this study.

I thank to my co-supervisor Prof. Dr. Ahmet Varilci for their valuable contribution during my thesis.

I want to thank specially R.A. Gürcan Yıldırım for his effort, kind help and support during the preparation of sample and carrying out experimental measurements.

I would like to thank all my friends, especially R.A. Esengül İplik and lecturer Gökçe Dişlen for their support and patience during the preparation of thesis.

Also, I am grateful to TÜBİTAK(The Scientific and Technological Research Council of Turkey) for its financial support during my education of Master of Science.

Finally, I would express my gratitude to my family for their endless support, encouragement and patience.

TABLE OF CONTENTS

LIST OF TABLES

LIST OF FIGURES

CHAPTER 1

INTRODUCTION

As the potential difference is occured between two ends of a metal, the conduction electrons found in the metal begin to move at a particular direction. During the movement of conduction electrons at a particular direction, the conduction electrons lose a portion of their energies by interacting lattice atoms. The less collision between lattice electrons and the conduction electrons are, the less energy they lose, and the more quickly they move. That is, the speed gained by conduction electrons is larger. Moreover, the conduction electrons moving faster form a larger current, and thus the resistivity of metallic structure is less. Additionally, if there is lattice imperfection stemming from structure in the metallic structure, the resistance faced by conduction electrons is larger. Therefore, if the metallic structure is cooled down below a certain critical temperature, the resistance faced by conduction electrons disappears and the conduction electrons move easily without interacting with lattice in the metallic structure. Besides, the resistance of metallic structure drops to zero under this critical temperature. For this reason, the material indicating zero resistivity under the temperature known as critical temperature,$T_{c,}$ is called superconductor. The first studies related with superconductivity had been started with the liquefaction of helium, whose boiling point is 4.2 K, by Kammerling Onnes in Leiden University in 1908 **[1].** After three years, in 1911, Onnes and his friends investigated platinum firstly, and they discovered that the resistivity of platinum was related with the materials purity.

Onnes and his friends measured the resistance of mercury known as the most pure material. While they expected that the resistance of mercury went to zero at 0 K, they observed that the resistance of mercury went down sharply to very small values, which was not measurable, about 4.2 K. This new event so-called perfect conductivity is named as superconductivity by Onnes and his friends **[2].** Onnes mostly examined the electrical and magnetic properties of superconductors at these studies conducted after this time. Approximately one year later, Onnes discovered that as the sufficient magnetic field was applied, the superconductivity disappeared. The liquefaction of helium and these experiments done at low temperatures brought Nobel Physics Prize to Onnes in 1913. Then, in Berlin in 1933, Walter Meissner and Robert Ochsenfeld investigated the magnetic features of superconductors; they discovered the diamagnetic feature of superconductors which is another one of the determining factor **[3].** That is, Meissner and Ochsenfeld observed that if the magnetic field is applied to the superconductor material expels this magnetic field. Similarly, the magnetic field was applied to the superconductor material after this material was cooled down under critical temperature, they noticed that the magnetic flux does not enter the superconductor material. Furthermore, they point out that the superconductor material lose superconductivity feature at magnetic fields being larger than critical magnetic field. In 1935, the equations explaining the thermodynamic properties of superconductivity like Meissner Effect and the penetration depth of flux into a superconductor were derived by Fritz and Heinz London brothers. These equations are also known as London equations in literature. This was the first semi-classical approximation to superconductivity **[4,5].** Until 1940's, the superconductivity researches focusing on the pure materials tended to metal oxides later. In 1950's, these studies tended to metallic and non-metallic alloys

intensively. London theory did not take into account the effect of quantum. In 1950, the first quantum mechanical approach was performed by Landau and Guinzburg **[6].** The theory put forward by Guinzburg and Landau maintained the existence of an order parameter between the normal state and superconducting state. This theory had been formulated terms equivalent of an order parameter to microscopic wave functions so as to explain superconductivity. That is, Ginzburg and Landau clarified the superconductivity by using a partial differential equation similar to Schrödinger equation. In 1957, J. Bardeen, L. Cooper and J.R. Schrieffer were able to reveal the microscopic theory known as BCS theory **[7].** The main theme of this theory is to form a related situation known as Cooper Pairs between two electrons. Moreover, in 1957, Alexei Abrikosov discovered a new type of superconductor category named as second type superconductors in Moscow **[8].** This type of superconductors is unstable because of the fact that they have negative surface energy in a magnetic field. Therefore, at superconducting state magnetic field was leaking to sample up to a certain magnetic field. This value exceeds, although the sample is still superconductor, the magnetic field partially penetrates into the superconducting material, and this statement forms mixed state in the sample. Superconductors, including the first and second type, are separated into two different categories with the discovery of mixed state by Abrikosov. In 1962, B.D. Josephson put forward that an electric current between two superconducting materials occurred even if this two superconducting were separated into a thin non-superconducting material or insulating material. This is another important theoretical development in superconductivity. This tunneling event is known as Josephson Effect today **[9].** The date of high temperature superconductivity started the discovery of $La_{2-x}Ba_xCuO_4$ whose critical transition temperature was measured as 30 K by Georg Bednorz and

Klaus Alex Müller in 1986 **[10].** In 1987, Mitchell and his friends discovered Bi-Sr-Cu-O superconductors, whose critical temperature is between 7–20 K **[11].** In the same year, superconductivity compound, $YBa_2Cu_3O_{7-x}$ (for x=0.1), having the critical temperature at 92 K was found by K. Wu Ashburn and Paul Chu **[12].** Due to the fact that the critical temperature of this compound was higher than boiling temperature of liquid nitrogen, 77 K, the researches done on the oxide superconductors had a great acceleration later. In 1988, Maeda and his friends added Ca to Bi-Sr-Cu-O system and the critical temperature of this system was measured as 110 K **[13].** Also, in 1988, Hazen and his friends discovered the critical temperature of Tl-Ba-Ca-Cu-O system as 120 K **[14].** As can be seen, all of the new superconductor materials having high critical temperature are copper oxides. In 1993, Schilling and his research group discovered $HgBa_2Ca_2Cu_3O_{1+x.}$ In Hg-Ba-Ca-Cu-O system, the highest critical temperature value,133 K, was obtained until now **[15,16].** Finally, in 2001, MgB_2 metal alloy superconductor, which was exciting the research groups all over the world, was discovered. Akimitsu and his friends announced at a meeting that MgB_2 metal alloy was superconductor at 39 K **[17].** The critical temperature of this system was found to be as 39 K. This system grabbed both theorists and the groups working experimental due to the fact that this system fitted with BCS theory.

CHAPTER 2

PROPERTIES OF SUPERCONDUCTIVITY

2.1 CRITICAL TEMPERATURE

The temperature losing the resistance of a conductor is called as the transition temperature of conductor or critical temperature. As shown in Figure 2.1, the metal resistance goes to zero after the transition temperature. There are two steps for the metal-superconductor transition statement of a material. These are the pieces grains being the characteristic property of granular structure and the interactions that result from bounding between pieces. As the material is exposed to the cooling process, these are pieces making the transition to superconductivity firstly, and the transition temperature coming from pieces are seen at the first step. The transition temperature to superconductivity has a temperature range like ΔT_c. This temperature range is the temperature difference between T_c^{onset} and T_c^{offset}. The temperature beginning the transition with the help of the superconductor pieces and beginning to lose the resistance of material is called as the first transition temperature(T_c^{onset}). The temperature, completed the superconductor transition all of the material and lost the resistance completely, is named as zero resistance transition temperature(T_c or T_c^{offset}).

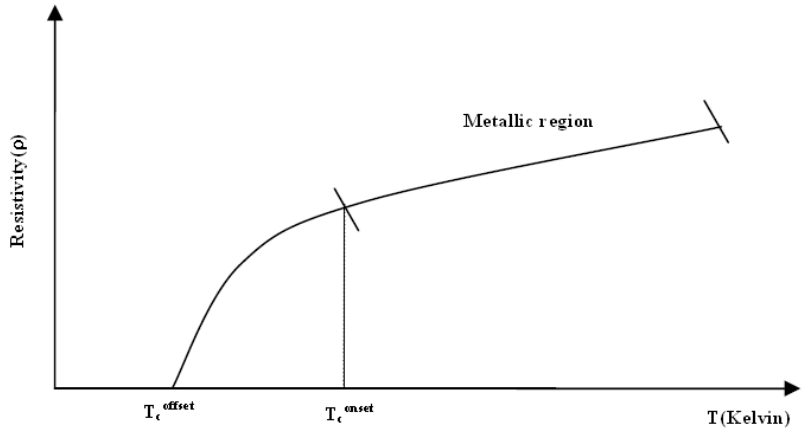

Figure 2.1: Variation of resistivity of a superconductor sample with temperature

Moreover, the superconducting properties for a sample can be determined with the aid of the width of the ΔT_c range. In this respect, ΔT_c difference defines the quality of sample. While the narrow interval shows that the sample is pure, quality, homogenous and single-crystal structure, the large interval points out that the sample is not pure. Although this interval is very narrow at the first type superconductors, this value is larger at the second type superconductors. Furthermore, the transition temperature is not usually very sensitive to against impurities at small amounts, the magnetic impurities decrease the transition temperature.

2.2 CRITICAL MAGNETIC FIELD

The another fundamental property determining the superconductor transitions as far as the critical temperature at least is the critical magnetic field. The magnetic field value applied to material at the start of the transition from superconducting state to normal state is called as critical magnetic field. As the external magnetic field is applied to superconductor material, the material maintains the superconductivity until a certain magnetic field value. Sufficiently strong magnetic field can destroy the

superconductivity and the normal resistance may occur. For a superconductor, the change of critic magnetic field as a function of temperature is shown in Figure 2.2.

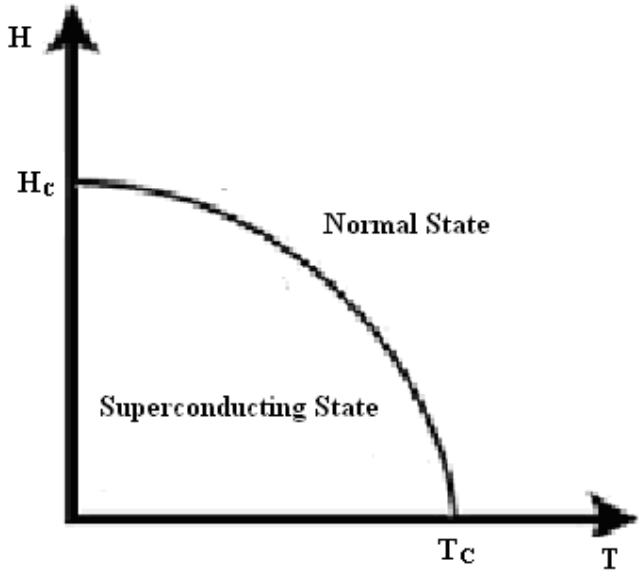

Figure 2.2: Variation of critical magnetic field H_c with temperature

The dependence of critical magnetic field on temperature is given by the Equation 2.1 **[1]**

$$H_c(T) = H_c(0) \times \left[1 - (T/T_c)^2\right] \tag{2.1}$$

Here, $H_c(0)$ is the maximum magnetic field required for the elimination of the superconductivity in material. If the applied magnetic field exceeds $H_c(0)$ value, the material can not be superconductor at any temperature. The critical magnetic field value at temperature(T=0°C) has a maximum value and at $T=T_c$ temperature this value goes to zero. This statement is the expected result because at $T=T_c$ temperature the sample is also normal state **[18].**

2.3 ZERO RESISTANCE PROPERTY

The most fundamental property utilized to identify the superconducting state is zero resistance property. The superconducting event and zero-resistance property firstly observed by German physicist H.K Onnes by doing studies about the electrical conductivity of metals at low temperatures in 1911. It was observed that the resistivity of mercury went to a limit value at 4.2 K at the studies done by Onnes. The resistivity was observed by Onnes is infinitesimal; that is, i.e. usually zero, under T_c. Onnes is right about the transition to a new state of materials under critical temperature and he explained this statement as superconducting event. Above the critical temperature ($T>T_c$), the material is the normal state; however, the material performs a transition to superconducting state under critical temperature ($T<T_c$) **[18].** This transition looks like another known phase transitions such as vapor-liquid transition at vaporization point or ferromagnetic transition at Curie point. The resistivity is zero below the critical temperature. This is shown in Figure 2.3.

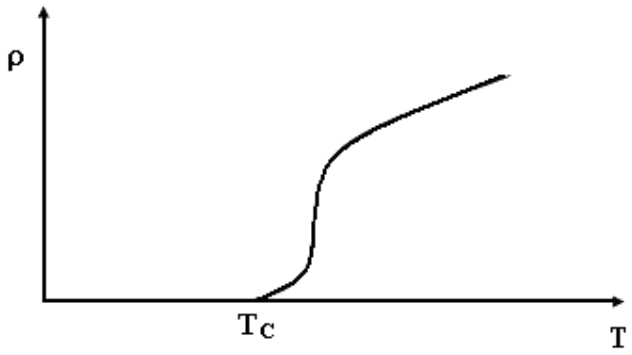

Figure 2.3: Variation of temperature dependence of resistivity of superconductor

The resistivity of a metal varies according to the free-electron model as shown in Equation 2.2.

$$\rho = \frac{m}{ne^2\tau} \tag{2.2}$$

Here, n is the electron density, m is mass, e is the electron charge, τ is the collision time, and the decrease of resistivity (ρ) points out the decrease of temperature. If the collision time has too large value at low temperatures, the resistivity (ρ) gets lost completely, and then this statement is called as superconductivity. The most common technique to measure the resistivity of a superconductor is to investigate the current passing through a loop-shaped metal ring as a function of time. If metal is normal state, current loses in metal quickly. If metal ring has zero resistance; that is, superconductor, current continues to flow at the first current value in ring without any decreasing at current value. The result of studies done by a lot of researchers indicated that the maximum value of the resistivity of superconducting lead ring is 10–25 ohm.m. Moreover, the superconductivity transitions of pure and impure samples are different from each other. As shown in Figure 2.4, if the sample not only consists of metallic elements but also is pure and perfect in terms of structure, the superconductivity transition is usually sharp **[19].**

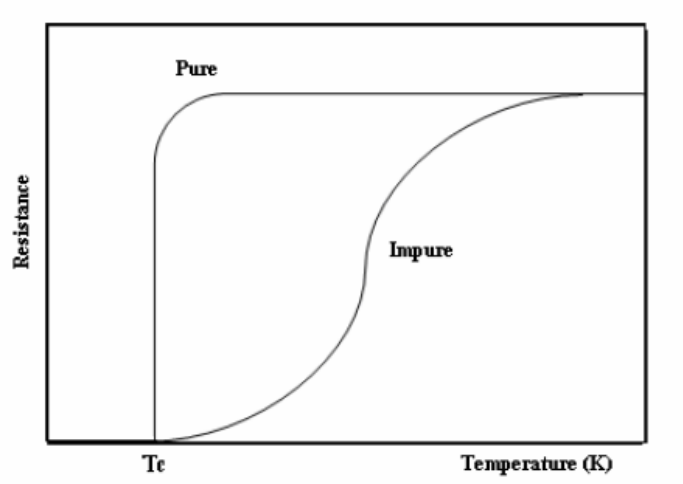

Figure 2.4: The graphics of temperature dependence of the resistivity at a temperature close to transition to superconductivity for pure and impure Sn metal

2.4 MEISSNER EFFECT

Until 1933, it was considered that the superconductivity was a special view of the perfect conductivity. The basic requirements to be a superconductor material are that it shows the properties of zero-resistivity and perfect diamagnet. In 1930's, experiments done to understand the magnetic properties of superconductors revealed different results. In 1933, Meissner and Ochsenfeld discovered that when a superconductor material is placed in a weak magnetic field, the magnetic field is expelled out from the material as being $\vec{B} = 0$ at every point of material. If a perfect conductor is cooled down below the critical temperature as there is a magnetic field, the magnetic field remains in the conductor even if the magnetic field is put out. The equilibrium thermodynamics is not applied in the perfect conductor because the final version of material in the magnetic field depends on whether the magnetic field is applied firstly or not. Due to the fact that the final version of material depends on the

order of making operation, the field is applied after cooled below T_c, it is required that the field is expelled from superconductor. On the other hand, the field is applied firstly, then the material is cooled below T_c, and the field is not expelled out from the superconductor. Thus, if the field is applied before the material cooling below T_c or after the material cooling below T_c, the same state; that is, $\vec{B} = 0$, is reached within the material. This effect is shown in Figure 2.5 for a spherical material. While the temperature is larger than T_c, the field penetrates the material as shown in Figure 2.5(a). Nevertheless, while the temperature is decreased below the critical temperature, the field lines are removed from superconductor as seen in Figure 2.5(b).

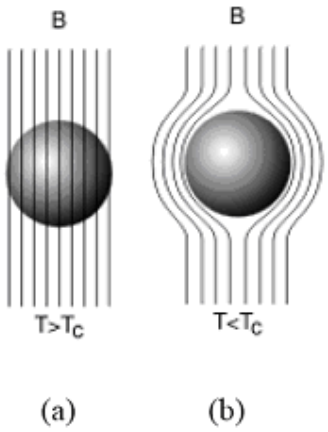

Figure 2.5: Meissner Effect a) Normal State b) Superconducting State **[18].**

In this respect, a superconductor is a material which is not only an excellent conductor but also an excellent diamagnetic substance. The effect being expelled out of magnetic field from superconductor is known as Meissner Effect. Being B=0 in a superconductor is a fundamental fact as much as the resistance of the material has zero resistance. If the applied field is increased like $B>B_c$, the superconducting state gets spoiled, and the field penetrates the sample.

Magnetic induction in a material is given as in Equation 2.3 below

$$\vec{B} = \mu_0 \cdot \left(\vec{H} + \vec{M} \right) = \mu_0 \cdot (1 + \chi) \cdot \vec{H} \tag{2.3}$$

Here, $\vec{H}$ is the magnitude of magnetic field, $\vec{M}$ is the magnetization in surroundings and χ is the magnetic susceptibility. When $\vec{B}$ is equal to zero in a superconductor at superconductivity statement, we can get this Equation 2.4 by means of the equation above.

$$\vec{M} = -\vec{H} \tag{2.4}$$

The means of Equation 2.4 is that the magnetization in sample is equal and opposite direction to the outer magnetic field. So, sample is diamagnetic and its susceptibility $\chi = -1$ **[18].** The change of magnetization in a superconductor with outer magnetic field is shown in Figure 2.6.

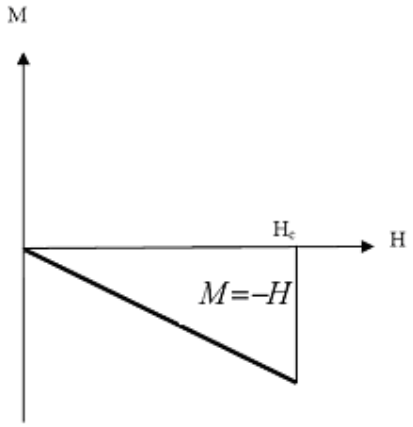

Figure 2.6: Variation of magnetization with magnetic field in a superconductor

2.5 PENETRATION DEPTH

As it is known, the excellent diamagnet of a superconductor occurs with the reset of passing flux. This event materializes with the help of the super-current flowing from the surface of superconductor. The thickness of super-currents flowing in the sample is called as the magnetic field penetration depth. In fact, these currents do not only occur on the surface of only a very thin layer of matter. In contrast, these currents are distributed over a thin layer with a thickness of 10–100 nm by penetrating from surface to material. If it is thought that the applied magnetic field is parallel to the surface of the sample, the magnetic field, $\vec{B}$, at thin layers varies with depth as equation 2.5 **[14]** given below

$$B(x) = B_0 e^{-x/\lambda} \tag{2.5}$$

Here, B_0 the value of the applied magnetic field on the surface, x the distance from the surface towards the inside of the sample, λ the penetration depth. As can be seen from this formula, as it has gone towards the inside surface of the superconducting, the field by decreasing as exponential. This statement can be shown in Figure 2.7 as below

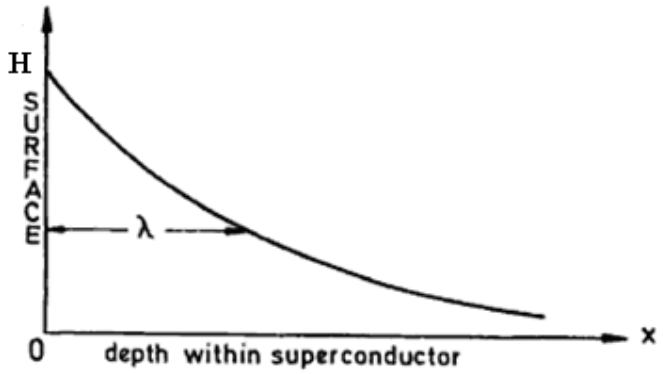

Figure 2.7: Schematic decay of applied magnetic field in the interior of a superconductor **[20].**

Thus, the magnetic field is zero in the sample in accordance with Meissner Effect. Moreover, the value of λ is typically between 10–100 nm. The penetration depth value is not fixed, which depends on temperature and type of material. The penetration depth varies with the temperature as Equation 2.6 shown below

$$\lambda(T) = \lambda_0 \left[1 - (T/T_c)^2\right]^{-1/2} \tag{2.6}$$

Here, λ_0 is the penetration depth at 0 K **[21].** Although the penetration depth at low temperatures is almost independent of temperature, it can be seen that this value is infinite at the temperature which is closer to T_c. In conclusion, the sample turns back to the normal state.

2.6 COHERENCE LENGTH

Another important parameter related with superconductivity is known as coherence length. The coherence length was firstly suggested by Pippard in 1953

[22]. Coherence length is thought as the smallest dimension on which the superconductivity is occurred or destroyed. In addition, according to BCS theory, the coherence length is directly related with the length in which the electrons of cooper pair stay together. If the coherence length in a pure superconductor is ξ_0, the temperature dependence of coherence length can be given as Equation 2.7 **[23].**

$$\xi = \xi_0 / (1 - T/T_c)^{1/2} \tag{2.7}$$

Coherence length is related with the metal whether pure or not. While the impurities and defects in metal increase the coherence length by decreasing the free path of electrons, they decrease the coherence length. That is, λ and ξ are inversely proportional to each other. The bigger the coherence length of material is, the better the superconductor is. The coherence length especially has an important place in determining the second type of superconductors. While the increasing of the proportion in λ/ξ put forward the second type superconductivity. Detailed analysis shows that the coherence length and penetration depth are related with the mean free path of normal metal electrons. The mean free path in metal can be shortened by adding impurities to metal. When the impurities are added to metal, the penetration depth increases, and then the coherence length decreases. The change of metal from first type to second type is provided by adding another metal to the metal.

2.7 GINZBURG-LANDAU PARAMETER

The first superconductivity theory put forward by Ginzburg and Landau described the phase transition at zero magnetic field. Ginzburg and Landau get

theoretically temperature dependent penetration depth λ and coherence length ξ. κ known as Ginzburg-Landau parameter is the ratio of these two lengths. This expression can be written as $\kappa=\lambda/\xi$. The value of κ has an important role in determining the superconductivity type of metal. If κ value is smaller than $1/\sqrt{2}$, first type superconductors are obtained. However, superconductors having k value above $1/\sqrt{2}$ are second type superconductors **[19].**

2.8 FORBIDDEN ENERGY GAP

One of the characteristic properties of the superconducting state is the energy gap. If we separated the superconducting state and normal state as basic state and excited state, these two states are separated with the energy range of 10^{-4} in magnitude. There is no state at this energy gap and the states on these ranges are not superconductor. The width of the energy gap is equal to the binding energy of Cooper pairs. The presence of energy gap can be proven by tunneling, photon absorption and the decrease of superconducting heat capacity. Moreover, as the material passes from normal state to superconductor the structure passes from non-uniform structure to uniform structure. Δ being described as the half of the energy gap is usually called as energy gap parameter or order parameter. The energy gap at superconductors is totally different from the energy gap at insulators. While the electron-lattice interaction dominates the energy gap being at insulators, the electron-electron interaction dominates in superconductors. The energy gap is approximately 1 eV in insulators, 0.1 eV in semiconductor and 10^{-3} eV in superconductors. If the temperature of superconductors is gone up towards T_c, the number of free electrons

increases. For this reason, the magnitude of energy gap continuously decreases, and all of the electrons are free at $T=T_c$. In this state, the energy gap, E_g, is equal to zero.

2.9 FIRST AND SECOND TYPE SUPERCONDUCTORS

The superconductor materials are classified into two groups as first and second type superconductors according to the behaviors in the applied magnetic field. While the pure samples of all elements except Nb and the materials fitting BCS model shows that the first type superconductivity properties, alloys and transition metals indicate the behavior of the second type superconductor properties. There is no difference in the superconductivity mechanisms of first and second type metallic superconductors. Both of them have similar properties in superconductivity-normal transition at zero magnetic field. There are surface currents at first type superconductors, and so these superconductors behave like a perfect diamagnet. However, when the applied magnetic field from outer exceeds the critical magnetic field value, the sample returns the normal state, and the superconductivity disappears. In this case, the external magnetic field penetrates the sample completely and the resistance of the sample will be different from zero. Here, transition of material to normal state is formed that increasing magnetic field energy, occurs at the end of the increasing outer magnetic field, equalize the energy difference between normal and superconducting states **[24].** Normal-superconducting transitions are sharp in the first type superconductors. Second type superconductors have a stronger structure mechanically compared with the first type superconductors. Second type superconductors that have two critical magnetic field values called as low H_{c1} and high H_{c2} expel the critical field value up to H_{c1}. The magnetic field between H_{c1} and

H_{c2} enters into the sample partially. The material is defined as mixed state at the magnetic field values between H_{c1} and H_{c2}. Nevertheless, the material still preserves the superconductivity property at this state. If the magnetic field value is bigger than H_{c2}, the magnetic flux penetrates to the material. Thus, the material loses the superconducting property, and the material returns the normal state. This situation is shown in Figure 2.8.

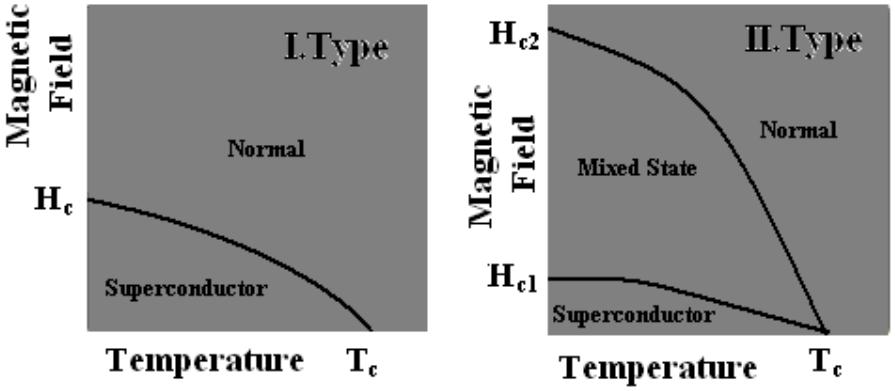

Figure 2.8: Temperature dependence of critical magnetic field a) for first type superconductors b) for second type superconductors

Another important difference between first and second type superconductors is that κ known as Ginzburg-Landau parameter is different for both type of superconductors. The coherence length is larger than penetration depth for the first type superconductors, and κ is smaller than $1/\sqrt{2}$ for first type superconductors. The situation for the second type superconductors is opposite form, which κ value is bigger than $1/\sqrt{2}$ **[19].** Besides, second type superconductors used in magnet construction due to the fact that second type superconductors have high critical

magnetic field value, and also they have an important role in technological applications.

2.10 FLUX QUANTIZATION

The flux quantization was suggested by Fritz London in 1950. Until 1950s, the quantization was only thought to be microscopic. Conversely, while London thought that the superconductivity is a basically quantum event, he suggested that the quantization is macroscopic. London came up with the idea that the quantization occurs in macroscopic dimension by setting the electron system at a superconductor, which has an advanced level correlation because the movement of electron pairs in superconductor material depends on the movements of others. For example, we consider that a superconductor persistent current circulates in a metal ring. The behavior of this current looks like the movement of electron in the orbital of atom. According to quantum theory, the quantity describing the state of such an electron takes the quantized values. While we encountered these microscopic quantization events that we could not observe directly in atom, we observed the quantization of electric current in a macroscopic quantity. Hence, it is shown that the current in a superconducting ring can not take continuous values, that is, it is discontinuous. Magnetic flux has also quantized values like electric current. As a result, the magnetic flux passing from superconductor ring, that is $\phi = BA$, had been quantized. What is more, including ϕ_0 is basic flux quantum and n is integer, the magnetic flux passing from ring is given as

$$\phi = n\phi_0 \tag{2.8}$$

ϕ_0 is found as hc/2e and London called fluksoid to ϕ_0. During the researches done by London, he had got a value above twice the magnitude of the value of ϕ_0. This is so because the superconductivity theory was being appeared by then.

2.11 BCS THEORY

The first true approaches to superconductivity were suggested by three American scientists John Bardeen, Leon Cooper and John Schriffer. They came up with a detailed theory known as BCS theory. The suggestions of BCS theory are in agreement with the experimental results perfectly. The main theme of this theory is that two electrons between which there is a kind of an attractive interaction form the connected pairs known as Cooper pairs. BCS theory intends to explain the net gravitational interaction between electrons where are in the narrow energy range close to the Fermi surface energy and the superconductivity near absolute zero. This theory indicates that not only the corner stone of superconductivity is electron pairs but also there is a second order phase transition. That is, the charge carriers in a superconductor are Cooper pairs, not the individual electrons like a normal conductor. BCS theory explains a number of observed events like zero resistance and Meissner Effect. To explain this statement, an instant was shown from the movement of electron between positive lattice ions Figure 2.9 below.

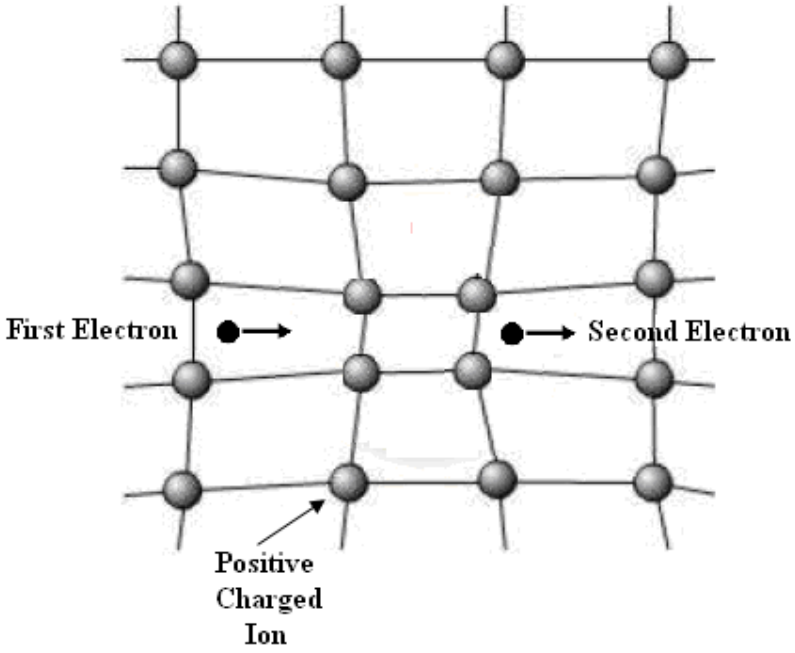

Figure 2.9: Schematic diagram of attractive interaction sourced from lattice deterioration

If we analyze this situation as shown in Figure 2.9, due to the movement of the first electron towards right side, + charged ions moves towards electron–lattice interaction. This leads to increasing the positive charge concentration at small amount. Moreover, another electron passing from that region, that is the second electron of Cooper pair, is received through the positive charged region, which is infected. The reason generating Cooper pairs is the electron-lattice-electron interaction between two electrons. Here, crystal lattice serves as mediator so as to occur an attractive force. Because of the fact that the quantized lattice vibration is called phonon, some scientists named this event as phonon mediation mechanism.

A Cooper pair consists of two electrons having equal but opposite momentum and spin. Two electrons, which are in connected state, are paired like a single system, and the movements of them are common. Cooper points out that these electrons are

close to Fermi surface. Thereby, if there is any current in a superconductor, Cooper pair occurs a system whose total momentum and spin are zero. Cooper pairs behave like bosons owing to the fact that their spins are zero, and all of them can be present in the same quantum state. The fundamental statement is established all of the electrons to form connected pairs at BCS theory.

BCS theory has been successful in explaining marked superconducting properties like zero resistance and flux exterior. Although BCS theory is successfully applied to a large portion of the low temperature superconducting materials, it is not available for high-temperature superconducting materials. If we look at the results of BCS theory, we can get

1) An attractive interaction between electrons can give up to ground state separated from excited state, and this energy gap is nearly 10^{-2} eV in magnitude **[24].**

2) The coherence length and the penetration depth brings about the natural consequence of BCS theory.

3) In fact, theory explains the behavior of superconductivity with the presence of energy range between ground state and excited state of macromolecules as shown in Figure 2.10.

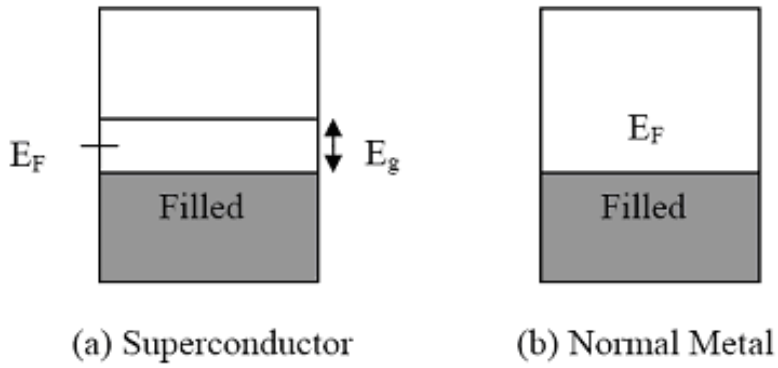

Figure 2.10: a) Energy gap at the Fermi level in the superconducting state b) Conduction band in the normal state **[21].**

As it is seen in Figure 2.10b, there is no energy range in normal conductor. Fermi energy in normal conductor represents the largest kinetic energy, which free electrons have at T=0 K. The energy range of a superconductor represents the energy which is necessary to break one of the Cooper pair. The energy range of a superconductor is an order of 10^{-3}. This value is very small compared with the semiconductor energy range, 1 eV, and the metal Fermi energy, 5 eV.

According to theory, the relation between energy range and transition temperature is in the form of $E_g=3.53\ k_bT_c$, and this is the dimensionless. This result is compatible with the experimental data in classical superconductors **[21].**

Hence, the higher energy range superconductors have, the higher higher critical temperature they have **[25,26].**

4) The magnetic flux through a superconducting ring is quantized, and the effective charge is 2e **[24].**

2.12 THE TRANSPORTATION OF CURRENTS IN SUPERCONDUCTORS

While the current in metals is moved by conduction electrons, in superconductors the current is carried by Cooper pairs. As the currents are moved in metals, the conduction electrons encounter with resistance. In superconductors, the resistance is zero. Two electrons of Cooper pair scatter with each other. Nevertheless, the momentum of electrons change at this scattering, the total momentum of pair remains constant. Owing to the fact that total momentum of pair does not change, the resistance does not occur, and thus also current does not change

so that no loss in current occurs. In order to change the current, the total momentum has to change. Moreover, the energy has to be given to the system to change the total momentum. This energy is required for the decomposition of electrons in Cooper pair. There is a current density which gives this energy to Cooper pair. This current density is called as critical current density. Cooper pairs separate the particles above the critical current density, and these particles behave like a normal electron. If these particles can carry the current, they can form the resistance. Cooper pairs responsible for superconductivity occur at the temperatures under the critical temperature, or they lead to the resistance via decomposition at the temperature above the critical temperature.

2.13 CRITICAL CURRENT

Critical current is described as the magnitude of current at the moment, when current meets with the resistance. Critical current is one of the important characteristic properties of superconductors and it is shown as I_c. Firstly, it can be seen that the total magnetic field value reaches the critical magnetic field, H_c, at any part of the surface resistance. The magnitude of critical current depends on the sample geometry and the structural properties of sample. If the magnitude of current exceeds the critical value, the resistance appears. In order to analyze this state, we consider a superconductor wire in cylindrical structure having r radius and passing through I current. According to Ampere's Law(Equation 2.9)

$$\int \vec{B}\, d\, \vec{l} = \mu_0\, \vec{I} \tag{2.9}$$

If B magnetic field surrounding the superconductor wire occurs, we can get Equation 2.10

$$\vec{B} \cdot 2\pi r = \mu_0 \cdot \vec{I} \tag{2.10}$$

If B value reaches the critical H_c value, the current in wire reaches the critical value. Because critical current can not be bigger than current forming the critical magnetic field. Figure 2.11 shows the phase diagram of critical current density variation of magnetic field and temperature. Critical current statement, wire loses superconducting property, and critical current is given Equation 2.11 below

$$\vec{I}_c = 2\pi r \vec{H}_c / \mu_0 \tag{2.11}$$

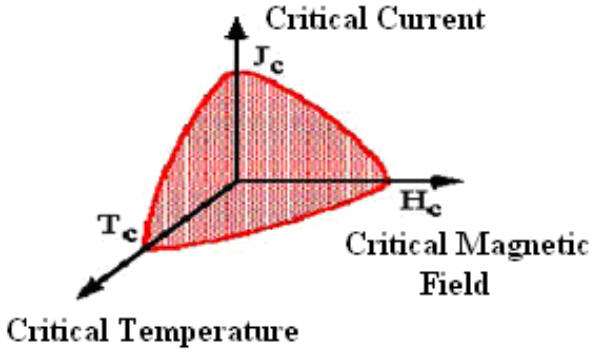

Figure 2.11: Critical surface phase diagram

It points out that the phase diagram showing the change of critical current density with magnetic field and temperature. The superconductor loses the zero

resistance when the critical field value exceeds H_c value. On this condition, critical current density and critical current are expressed as Equation 2.12

$$I_c = 2\pi r B_c / \mu_0 \text{ and } J_c = 2B_c / \mu_0 r \quad (2.12)$$

Moreover, when the current density in a superconductor exceeds the value called as critical current density(J_c), the superconducting state loses. This statement is called as Silsbee Effect **[27].**

2.14 TUNNELING AND JOSEPHSON EFFECT

If two superconductor materials are separated from each other with very thin insulating layers shown in Figure 2.12, the current can pass through the insulating layer even if a very small potential difference occurs **[28].** In 1961, in addition to the single particle tunneling, Brian Josephson came up with the idea of tunneling of Cooper pair **[9].** Josephson predicted that the pairs form DC current via tunneling without encountering any resistance. Furthermore, this current forms without applying any potential difference. Besides, Josephson showed that as potential difference is applied to the joint, an ac current can appear as a second incident. When the superconductor sample is separated with a thin insulator, Cooper pairs do not pass from the first Fermi surface of superconductor to the second Fermi surface of superconductor. While a very small voltage is applied to one of superconducting parts, the electron concentration at this part increases, and then electrons will tend to pass through another superconducting part. However, there is a limit value for applied voltage and if this limit value exceeds, the tunneling effect disappears. This

transition is only possible with tunneling. That is, the electrons pass through with quantum mechanical tunneling. This state is known as Josephson Effect in superconductivity. During tunneling, energy has to be conserved; that is, all energy of system has to be same before and after tunneling. In addition, the distance between two superconductor materials for tunneling has not to be very large, and this distance has to be order of coherence length for superconductor. Moreover, experimental results show that the probability of tunneling is the same for Cooper pairs and single particles. Whereas tunneling gives DC current at zero potential difference, it gives AC current as the potential difference is applied. Therefore, tunneling effect is called as DC and AC Josephson Effect **[29].**

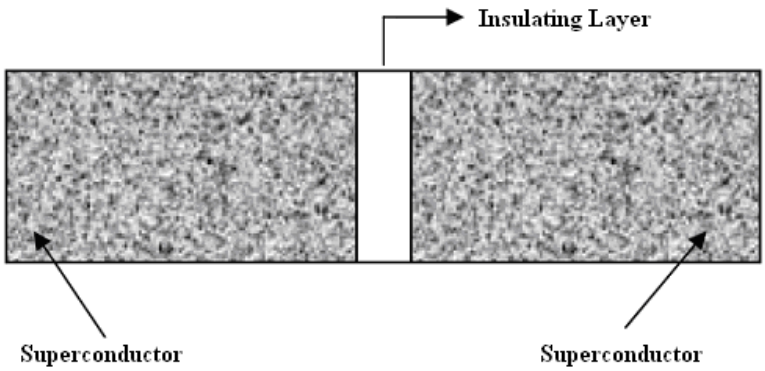

Figure 2.12: Two superconductor materials seperated with an insulator

2.14.1 DC Josephson Effect

The structure consisting of two superconductors separated with a thin oxide layer in 1-2 nm thickness is known as Josephson joint. Then, we consider a joint like this. All of the electron pairs in a superconductor have the same phases. As an external voltage is applied to two identical superconductors and the temperature is above absolute zero, the tunneling probability to both directions is equal to each

other. Therefore, a net current is not observed. Whereas, if two different superconductors form a joint, the current passes through joint, or not a potential difference is not applied. On this condition, the tunneling effect occurs in pairs by electrons. In this way, the current passing through without any potential difference is called as Josephson current. Also, this current is determined with the aid of the phase difference of wave function of electrons, which is in superconducting layers forming the joint. This phase difference can be expressed as shown Equation 2.13

$$\phi = \phi_1 - \phi_2 . \tag{2.13}$$

This is so, because the phase difference of Cooper pairs in both sides enables a current to occur. We can explain this situation as follows: The pairs can be represented with a wave function in superconductors as Equation 2.14 given below

$$\Psi = \Psi_0 e^{i\Psi} . \tag{2.14}$$

Here, Ψ_0 defines the phase, which is the same for each pair. It was observed that as the phase of one of the superconductors at joint is Ψ_1 and the phase of another is Ψ_2, an excessive current passing from the joint at zero potential difference as shown in the Equation 2.15 below

$$I_s = I_m \sin(\Psi_2 - \Psi_1) = I_m \sin\delta . \tag{2.15}$$

Here, I_m shows the maximum current passing through joint at zero potential difference. I_m value depends on the area of contact surface of superconductors, and this value decreases with the thickness of oxide layer exponentially **[9,21].**

2.14.2 AC Josephson Effect

When a potential difference is applied to joint consisting of different superconductors, it emits an electromagnetic waves, which can be determined experimentally like any ac circuit. If V potential difference is applied to joint, the electron pairs will pass through insulating layer, and they will gain 2 eV worthy of energy. Moreover, due to the fact that it does not spend energy in current transition, the energy gained by electron pair will radiate as light quantum at frequency of 2 eV/h. This radiation can be observed experimentally. As the AC voltage is enforced to one of superconductive parts, sinusoidal current flows through joint. This ac current produces an ac current which is given equation

$$I = I_m \sin(\delta - 2\pi ft). \tag{2.16}$$

Here, δ is the phase at t=0, and it is constant, f is the frequency of Josephson current given with 2eV/h **[9,21].**

2.15 HIGH-TEMPERATURE SUPERCONDUCTIVITY

All superconductors discovered before and after 1986 without including Cu-O plane are named as conventional or low-temperature superconductors. High-

temperature superconductivity expression is used for superconductors which have a layered structure including Cu-O plane regardless of T_c value. Until now, five fundamental hig temperature oxide superconductors such as La-Ba-Cu-O, Y-Ba-Cu-O, Bi-Sr-Ca-Cu-O, Tl-Ba-Ca-Cu-O and Hg-Ba-Ca-Cu-O are discovered and studied **[30].** However then, the highest known critical temperature for Hg layered superconductor system is increased up to 166 K. Y-Ba-Cu-O, Bi-Sr-Ca-Cu-O and Tl-Ba-Ca-Cu-O oxide superconducting systems are suitable for practical applications due to the fact that they cen be superconductors at liquid nitrogen temperature **[31].** As can be seen from high-temperature superconducting systems, almost all of the materials having high T_c include Cu-O layer. It is seen that there is a directly relation between the number of Cu-O layers and the critical temperature. The addition of Cu-O layers increases T_c value until the structure repeats itself periodically. Accordingly, it is expected that being added of extra Cu-O layer to this complex oxides brings out the critical temperature to higher values. It is certainly known that the maximum value of super currents is high at Cu-O planes and is very small at perpendicular to these planes. Moreover, the current density is much lower in bulk ceramics due to factors such as boundary effects. There are grains, in which the current flows very well, and impurities, acting like a dielectric at the grain interface in these materials. For this reason, the current has to pass through not only grains but also borders separated by the grains. Hereby, the current between grains only passes through via Josephson Effect known as weak band behavior. Due to the fact that the coherence length is very smaller than penetration depth at high temperature superconductors, almost all of these materials are second type superconductors. Despite the lower critical magnetic field value of high-temperature superconductors, B_{c1}, is low, the upper critical magnetic field value, B_{c2}, is high. That's why, the

fixing of magnetic vortexes weakens, and this situation leads to decreasing the critical current I_c. The magnitude of energy- barrier is smaller than conventional superconductors at new oxide superconductors. Furthermore, it is determined that small coherence length causes small energy barrier. In contrast to almost all of the low-temperature superconductors, it is seen that there is high spatial anisotropy at high-temperature superconductors. Bi layered superconductors are more anisotropic than La and Y layered compounds. Anisotropy stems from layered crystal structure assumed to be essential for high-temperature superconductivity. Scientists doped various rare-earth element ions to high-temperature superconductors. It was found that although some of this changes increase T_c, some of them decrease T_c. An important difference between high-temperature superconductors and low temperature superconductors is that the high temperature superconductors are not homogenous. The properties such as free pore, high density, strong connection between grains and homogenous structure which can be shaped are important. It is well-known that these new copper oxide superconductors have two distinct features like zero resistance and diamagnetism. In addition to these, it is pointed out that these materials have some properties written in below:

1) These materials are second type superconductors, whose upper critical magnetic field is larger than 100 T.

2) These materials are extremely anisotropic; that is, they have properties depending on the direction.

3) These materials are granular or ceramics structures. They have unsuitable mechanical properties like being inelastic and fragile owing to the fact that they are in ceramics structure.

4) Placing other atoms instead of the atoms at copper-oxide layers disturbs the superconductivity.

5) The properties such as band gap, high-temperature resistivity, critical current density, critical magnetic field are different.

6) The critical current density is very small for bulk and multi-crystalline structure materials.

2.16 HIGH-TEMPERATURE SUPERCONDUCTORS

Scientists have tried to find materials showing superconductivity at higher temperatures for years. Until now, it is known that the material having the highest critical temperature is Nb_3Ge **[32]** thin films, whose T_c is nearly 23.3 K **[33,34]**. As for various theoretical expectations, the critical temperature of superconductors for which the electron-lattice interaction is important is nearly 30 K. At the beginning of 1986, two scientists, J. George Berndnorz and Karl Alex Muller, made an important discovery about superconductivity in Zurich IBM Research Laboratory. These scientists found that the ceramics in which lantan, barium and copper were at mixed state points out the superconducting property at near 30 K **[10].** After this, the studies done in other laboratories, it was found that the superconductor phase is $La_{2-x}Ba_xCuO_y$ for x=0.2. Due to the fact that such high critical temperature is not expected for especially metal oxides, news related with high-temperature superconductivity. After a short period of time, the researchers raised the critical temperature value to 36 K by placing strontium instead of barium **[35].** Scientists inspired from this development made an effort in order to discover the materials having high T_c. The studies conducted on the superconductor behavior of metal

oxide have gained acceleration recently. It can be considered that the beginning of the studies done in high-temperature superconductivity was in 1986. At the beginning of 1987, the research groups in University of Alabama and Houston notified that they observed the superconductivity at a mixed phase consisting of yttrium, copper and oxygen at a temperature close to 92 K **[12].** Moreover, the superconductor phase was determined as $YBa_2Cu_3O_{7-\delta}$ by confirming from other groups around the world. By looking the ratios of barium yttrium and copper, this compound is named as 1:2:3 or Y-Ba-Cu-O **[36–39].** The transition temperature of this compound is over the boiling point of liquid nitrogen, 77 K. In this regard, this discovery was a milestone for high-temperature superconductivity. Recently, many complex metal oxides in ceramics structure were investigated, and the values over 100 K were observed for critical temperature. Mitchell et al. found the superconductivity in Bi-Sr-Cu-O system **[11].** In 1988, Maeda and his group observed superconductivity at 105 K by adding calcium to this system as Bi-Sr-Ca-Cu-O **[13].** Moreover, Tokano and his group found this superconductor at 110 K, by adding lead to the system **[40].** Addition of lead to system increases the ratio of the phase having high critical temperature. In 1992, Quidwai and research group found that the transition to superconductivity is at 130–140 K by adding antimony to the system **[41].** In 1993, Schilling and his research group observed superconductivity in mercury barium calcium copper oxide $HgBa_2CaCu_3O_{1+x}$ compound at 133 K; similarly, Chu and his group noticed superconductivity in high pressure with Hg based compounds at 150 K **[42,43].** After 1933, the highest critical temperature was got at 133 K in 1995 at normal pressure by using Hg-Tl-Ba-Ca-Cu-O compound. Almost all of high Tc superconductor materials are copper-oxide compound. The superconducting compounds investigated particularly

until now can be classified from types of crystal structures called as perovskit. The first class is cubic perovskit like $BaPb_{1-x}Bi_xO_3$. As known, this material is one of the first high T_c materials, whose transition temperature is 10 K. The second class known as $KNiF_4$ structure is a layered perovskits having tetragonal structure. An example for this class is $La_{1,85}Sr_{0,15}CuO_4$ having the transition temperature is nearly 38 K. The last class is multi-layered perovskits having orthorhombic structure such as $YBa_7Cu_3O_7$(T_c≈92 K). The crystal structure of these materials is described as CuO_2 plane and perovskit structure having missing oxygen. This material has a strong anisotropy; that is, it has a direction susceptibility at superconducting properties. Efficient super-currents flows throughout CuO_2 planes connected to each other with Josephson pairing. The carrier density of high-temperature superconductors is approximately two times of low-temperature superconductors. Coherence length is smaller than low-temperature superconductors and it varies according to the direction of the plane. That is, it has to change nearly 3 Å perpendicular to CuO_2 plane, nearly 10 Å through this plane. We can say that not only the maximum super-currents are high at Cu-O planes but also the maximum super-currents are much small at perpendicular to these planes.

2.16.1 The Crystal Structure of La-Ba-Cu-O(LBCO) Compounds

LBCO is the first high-temperature superconductor. The general formula of this superconductor system is $La_{2-n}Ba_nCuO_{4-y}$. The highest transition temperature of this La layered compound was obtained as near 35 K. Besides, when strontium and calcium are placed instead of barium at this system, it is observed that these elements show the properties of barium at superconductor compounds.

2.16.2 The Crystal Structure of Y-Ba-Cu-O(YBCO) Compounds

YBCO is the first superconducting material showing the transition temperature over liquid nitrogen temperature and cooled with liquid nitrogen. The general formula of the most studied stable compounds belonging to this superconductor system is $YBa_2Cu_3O_{7-n}$. These superconductor compounds are very sensitive to oxygen stoichiometry, and correspondingly these superconducting compounds have different physical structure and properties. While for n=0 the transition temperature of $YBa_2Cu_3O_7$ compound is 72 K, for n=1 the transition temperature of $YBa_2Cu_3O_6$ compound is nearly 60 K.

2.16.3 The Crystal Structure of Bi-Sr-Ca-Cu-O(BSCCO) Compounds

The first superconducting material consisting of Bi was obtained with the discovery of Bi-Sr-Cu-O by Mitchell and his friends in 1987 **[11].** After this discovery, Maeda and his friends increased the transition temperature from nearly 20 K to 110 K by adding Ca to this system. The general formula of this system which does not contain any rare element is given by $Bi_2Sr_2Ca_{n-1}Cu_nO_{2n+4}$ **[44].** Here, n is the number of copper oxide layers. If n value increases, critical temperature(T_c) value increases directly **[45].** These system has three different compounds as appropriate to chemical formula such as n=1,2,3. These compounds are $Bi_2Sr_2CuO_6$, $Bi_2Sr_2CaCu_2O_8$, $Bi_2Sr_2Ca_2Cu_3O_{10}$, and they are named as (2201), (2212), (2223) phases with respect to the proportion cations as following Bi: Sr: Ca: Cu: O. As shown from compounds, n denotes the number of Cu-O planes. At these systems, it

is known that the superconducting transition temperature goes up with the increasing of Cu-O layers. The superconducting transition temperature of these compounds, T_c, depends on the number of two-dimensional CuO_2 planes. Except for the number of CuO_2 and Ca planes, all superconducting compounds are structurally identical to each other. One of the general structural characteristic of BSCCO systems is that it is difficult to get these compounds as a single phase. Another feature is that the result stoichiometry can be considerably different from onset stoichiometry. Mixed phase property which makes even a single grain BSCCO system distorted and complex structure. This distortion and mixed phase properties affect all of the features of these systems such as critical temperature, critical current density, critical magnetic field, and the like. It is well-known that the superconducting Bi-layered compounds are quietly sensitive to onset composition, preparation procedures, sintering time and sintering temperature. As they can be all of the high-temperature superconducting systems, these compounds indicate a high anisotropy owing to the fact that lattice parameter c is relatively greater in accordance with lattice parameters a and b at the crystal structure of BSCCO systems.

2.16.3.1 The Crystal Structure of $Bi_2Sr_2CuO_6$ Compound

The superconducting system which does not contain Ca was firstly found as $Bi_2Sr_2CuO_6$ compound. $Bi_2Sr_2CuO_6$ compound was formed with respect to n=1 at the general series of $Bi_2Sr_2Ca_{n-1}Cu_nO_{2n+4}$, and also this compound was called as semiconductor phase or (2201) phase. Figure 2.13 indicates the crystal structure of $Bi_2Sr_2CuO_6$ compound. There is one CuO_2, two SrO and two Bi_2O_2 planes at the unit cell of crystal forming (2201) compound. CuO_2 plane takes place between two SrO

planes and two Bi_2O_2 layers. The formation order of these layers is in the form of Bi_2O_2-SrO-CuO_2-SrO-Bi_2O_2. One Cu atom composes square layered octahedral structure with six neighbor oxygen atoms. It is suggested that (2201) phase generates body-centered tetragonal structure, which has the unit cell dimensions such as a=b=5.4 Å and c=24.4 Å, or this phase generates deteriorated orthorhombic symmetry, which has the unit cell dimensions such as a=b=3.9 Å and c=24.4 Å **[46,47].**

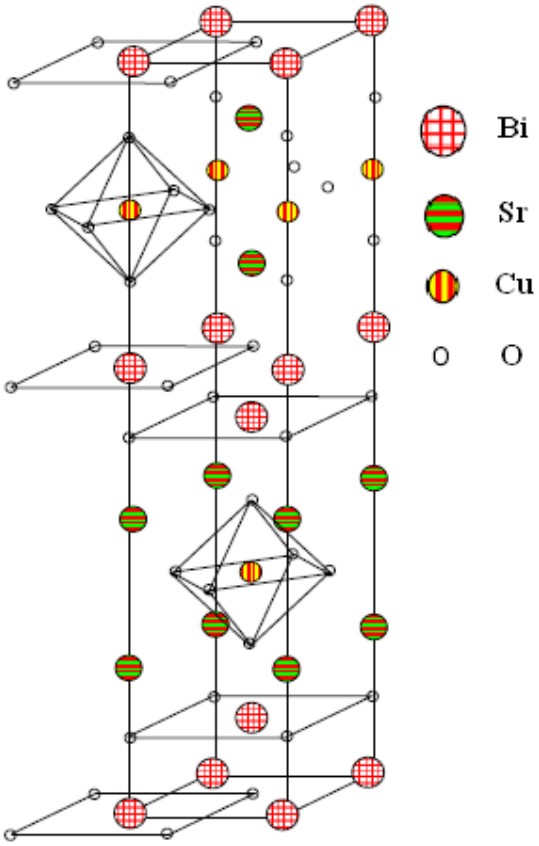

Figure 2.13: Crystal structure of $Bi_2Sr_2CuO_6$ compounds **[48].**

2.16.3.2 The Crystal Structure of $Bi_2Sr_2CaCu_2O_8$ Compound

$Bi_2Sr_2CaCu_2O_8$ is a compound, forming with respect to n=2 at the general series of $Bi_2Sr_2Ca_{n-1}Cu_nO_{2n+4}$ and called as low-temperature phase. Maeda and his friends were found the critical temperature of (2212) phase as 85 K by adding Ca to this triple that forms (2201) phase **[13].** Figure 2.14 indicates the crystal structure of $Bi_2Sr_2CaCu_2O_8$ compound. At the unit cell of crystal forming this compound, in addition to planes forming (2201) compound a $CaCuO_2$ layer takes part in, which settles among SrO planes. The formation order of these layers is in the form of Bi_2O_2-SrO-CuO_2-Ca-CuO_2-SrO-Bi_2O_2. Each of Cu atoms at this compound generates square layered pyramid form together with five neighbor oxygen atoms. There are 15 atoms at the unit cell of crystal. The lattice parameter of this compound, whose critical temperature varies among 75–85 K **[44]**, are given as a=b=5.14 Å and c=30.9 Å. It is suggested that the crystal symmetry is orthorhombic or tetragonal **[46].**

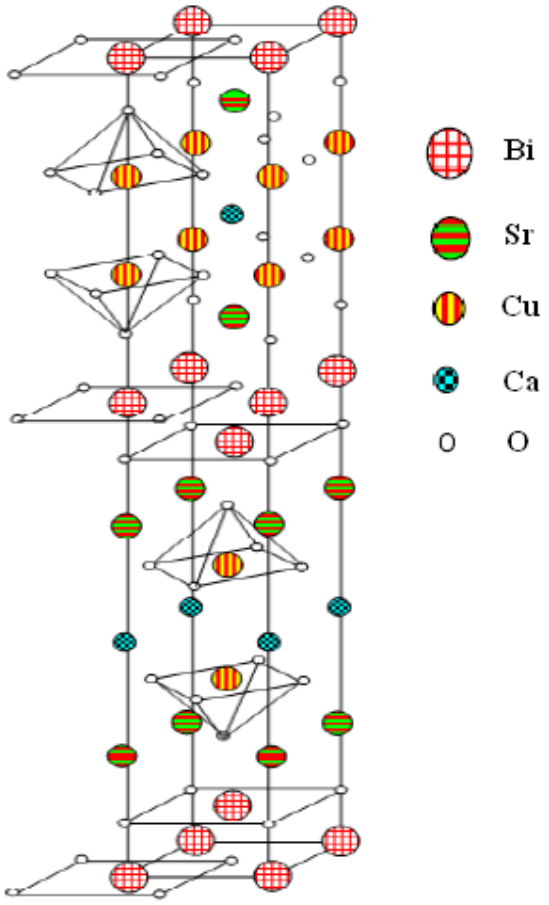

Figure 2.14: Crystal structure of $Bi_2Sr_2CaCu_2O_8$ compounds **[48].**

2.16.3.3 The Crystal Structure of $Bi_2Sr_2Ca_2Cu_3O_{10}$ Compound

This compound forms in accordance with n=3 at the general series of $Bi_2Sr_2Ca_{n-1}Cu_nO_{2n+4}$, and it is also called as high-temperature phase(2223). The critical temperature was observed 110 K by adding lead to the system **[40].** Figure 2.15 indicates the crystal structure of $Bi_2Sr_2Ca_2Cu_3O_{10}$ compound. There is a $CaCuO_2$ addition to planes being (2212) phase crystal structure at this compound having the highest critical temperature value. Each of these CuO_2 planes is separated from another with a Ca plane, which does not contain oxygen. As for the formation of these layers, it is in the form of Bi_2O_2-SrO-Ca-CuO_2-Ca-CuO_2-SrO-Bi_2O_2. (2223)

compound has the planes including two different Cu atoms. Cu atoms being in center were coordinated in two dimensional square lattice form by combining with four neighbor oxygen atoms. There are totally 19 atoms at the unit cell of the crystal **[49–51].**

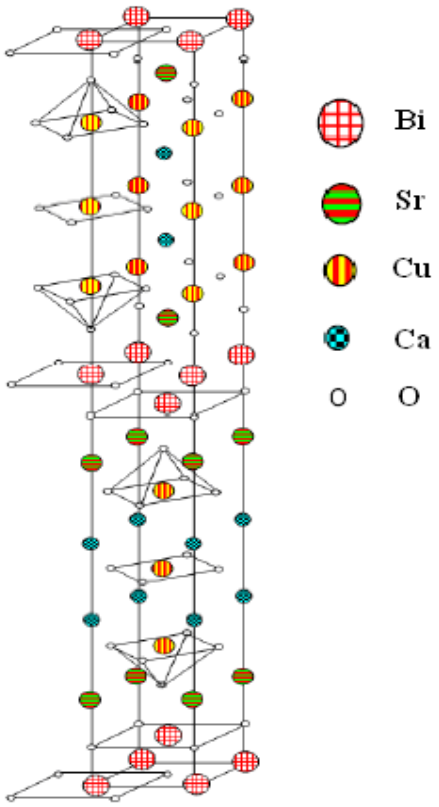

Figure 2.15: Crystal structure of $Bi_2Sr_2Ca_2Cu_3O_{10}$ compounds **[48].**

2.16.4 The Crystal Structure of Tl-Ba-Ca-Cu-O(TBCCO) Compounds

After discovery of BSCCO superconductor systems, Sheng and Hermann found Tl–Ba–Ca–Cu-O system whose transition temperature is above 100 K **[52].** Afterwards, Hazen and his friends formulated this system in the form of $Tl_2Ba_2Ca_{n-1}Cu_nO_{2n+4}$, and also the highest transition temperature of this system was observed for n=3 at 120 K. The transition temperature for other n values is 80 K for n=1(2021

phase) and 110 K for n=2(2122 phase). Despite Tl-Ba-Ca-Cu-O and Bi-Sr-Ca-Cu-O systems have the same crystal structure, they have different superconducting properties. Furthermore, thallium is not preferred so much because of the fact that thallium is a poisonous element.

2.16.5 The Crystal Structure of Hg-Ba-Ca-Cu-O(HBCCO) Compounds

The first superconducting material including mercury was discovered by J. N. Putilin and his friends in 1993 **[53].** The transition temperature of this superconducting system containing only one copper-oxide plane was obtained as 94 K. After A. Schilling and his friends observed that the transition temperature of this system was 130 K by adding Ca to the system, Gao and his research group increased the transition temperature to 133 K. Nowadays, the critical temperature can be increased to 166 K by means of the pressure applications. Schilling and his friends determined the lattice parameters of this structure as a=b=2.7 Å and c=16.1 Å, and also they found that the structure of this system is tetragonal.

CHAPTER 3

EXPERIMENTAL METHOD

3.1 SAMPLE PREPARATION

The solid state reaction method is the most common sample preparation technique for ceramic superconductors **[54].** $Bi_2Sr_2Ca_1Cu_2Ce_xO_y$ samples were prepared by the solid state reaction method. Molecular weights, symbol and purity of starting materials were given in Table 3.1.

Powder Name	Symbol	Purity(%)	Molecular Weight (g/mol)
Bismuth Oxide	Bi_2O_3	99.9	465.96
Strontium Carbonate	$SrCO_3$	99.9	147.63
Calcium Carbonate	$CaCO_3$	99.9	100.09
Copper Oxide	CuO	99.9	79.55
Cerium(IV) Oxide	CeO_2	99.9	172.20

Table 3.1: Symbol, purity and molecular weight of the compounds

Powders forming the composition were weighed in a precision microbalance(Figure 3.1). Then were mixed in a grinding machine for 48 hours except CeO_2. As a result of this, powder composition placed into a programmable tube furnace PROTHERM-MODEL PTF 12/75/200(Figure 3.2) for calcination process. The mixed powders were calcined in air at 830 °C for 48 hours. The heating and cooling rates of temperature for calcination process were applied 3 °C/min. Moreover, the steps of calcination process were shown in Figure 3.3.

Figure 3.1: XR 205SM-DR Precisa balance

Figure 3.2: PROTHERM (Model PTF 12/75/200) programmable tube furnace

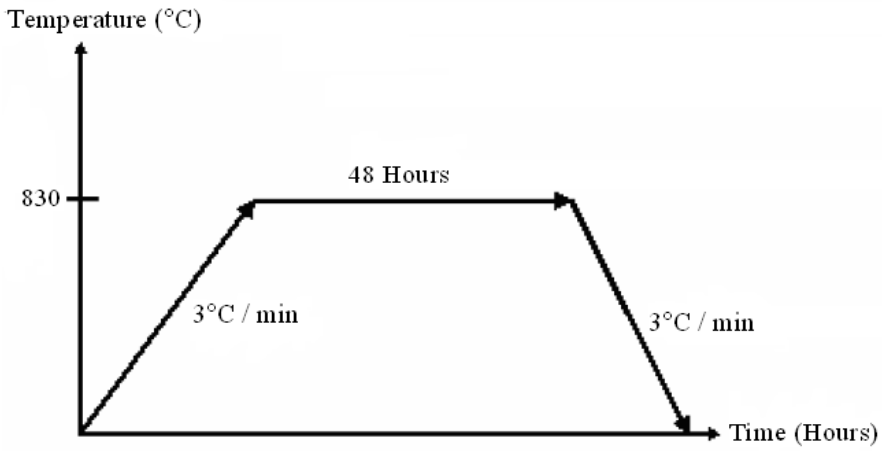

Figure 3.3: Calcination process of the samples

After calcination process, CeO_2 powders were weighed carefully in a precision microbalance. During regrind process, addition material, CeO_2, was added to mixture for eight different molar concentration of Ce such as 0, 0.001, 0.003, 0.005, 0.01, 0.03,0.05, 0.1. Also, for each different molar concentration, the mass of each composition was arranged as 4 g. totally. Then, each of composition was seperately mixed in agate mortar approximately half-hour by adding acetone. The

regrind materials were reground and pressed into rectangular bars of 10x4x2 mm^3 at 300 MPa with a hydraulic press(Figure 3.4). Afterwards, pellets were placed into a programmable tube furnace PROTHERM-MODEL PTF 12/75/200(Figure 3.2) for sintering process. The mixed powders were sintered in air at 830 °C for 48 hours. The heating and cooling rates of temperature for sintering process were applied 5 °C/min. Also, the steps of sintering process were given in Figure 3.5.

Figure 3.4: TSEK TÜMAS press machine

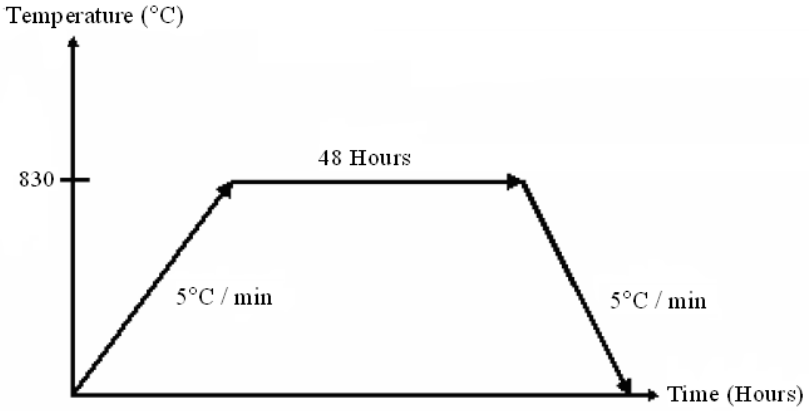

Figure 3.5: Sintering process of the samples

3.2 EXPERIMENTAL MEASUREMENTS

3.2.1 X-Ray Diffraction(XRD) Analysis

X-Ray Diffraction Analysis is an important method which is used not only to be investigated the crystal structures of samples but also to be determined the crystal phases. X-ray powder diffraction patterns were obtained by means of computer controlled Rigaku D/Max-IIIC diffractometer (CuK_α = 1.5405 A) in the range 2θ=3° - 60° (at 40 kV and 3 mA) with a scan speed of 3°/min.

Figure 3.6: Rigaku X-Ray diffractometer

3.2.2 Scanning Electron Microscopy(SEM) Analysis

Scanning Electron Microscopy(SEM) analysis is an important technique which is used to be investigated the microstructure of materials by scanning the surfaces. Scanning Electron Microscopy system is completely digital system so that it works with computer control. The surface morphology and microstructure of the materials were analyzed by Scanning Electron Microscopy(SEM), JEOL 6390-LV (Fig. 3.7). The magnifications to get information about the grains clearly were adjusted to be 8000.

Figure 3.7: JEOL JSM-6390LV scanning electron microscope

3.2.3 Electrical Resistivity Analysis

In this part of the measurements, resistivity measurements of samples were obtained with four probe method. This method involves setting four, equally-spaced point contacts down on the surface of a sample. The probe array of this method on a sample can be shown in the Figure 3.8 below. If we mention about the probes, two outer probes are used for current source. Conversely, two inner probes are used for measuring the resulting voltage drop across the surface of the sample. We measured temperature (30–150 K) and DC magnetic field (0 T,0.3 T, 0.7 T,1 T, 3 T, 5 T, 7 T) dependent of resistivity with 1 mA DC current in a cryostat.(Figure 3.9)

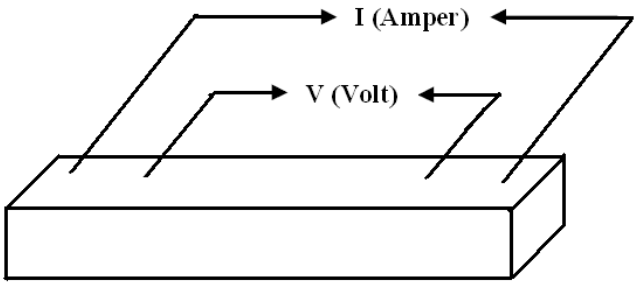

Figure 3.8: Schematic diagram of four probe method

Figure 3.9: Cryostat system

CHAPTER 4

RESULTS AND DISCUSSIONS

4.1 INTRODUCTION

In this chapter, resistivity measurements, X-Ray Diffractometer(XRD) and Scanning Electron Microscopy(SEM) analysis of $Bi_2Sr_2Ca_1Cu_2Ce_xOy$ (x=0, 0.001, 0.003, 0.005, 0.01, 0.03, 0.05, 0.1) samples were investigated, and the results of all measurements were discussed.

4.2 RESISTIVITY MEASUREMENTS

Resistivity measurements belonging to $Bi_2Sr_2Ca_1Cu_2Ce_xO_y$ samples prepared with the help of solid state reaction method were performed under various DC magnetic field values (0 T, 0.3 T, 0.7 T, 1 T, 3 T, 5 T and 7T) with 1 mA DC current in a cryostat. The resistivity-temperature graphs for these samples were shown in Figure 4.1– 4.8 below.

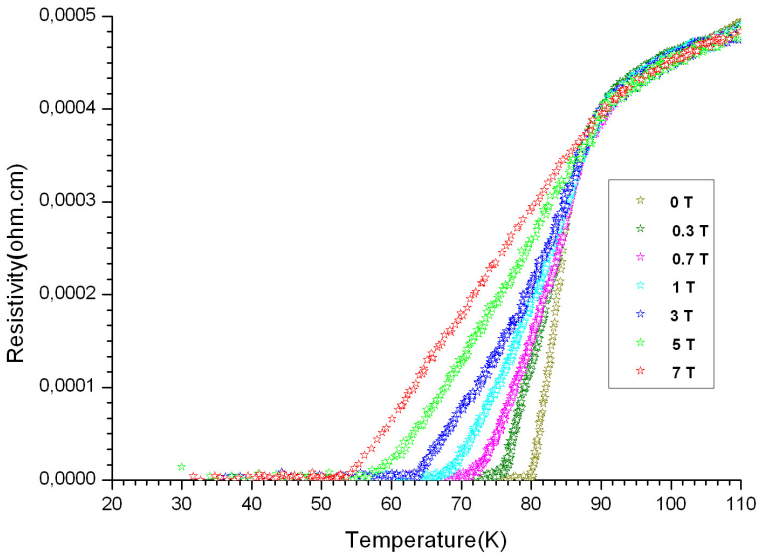

Figure 4.1: Resistivity versus temperature graph of $Bi_2Sr_2Ca_1Cu_2Ce_xO_y$ sample for x=0.0

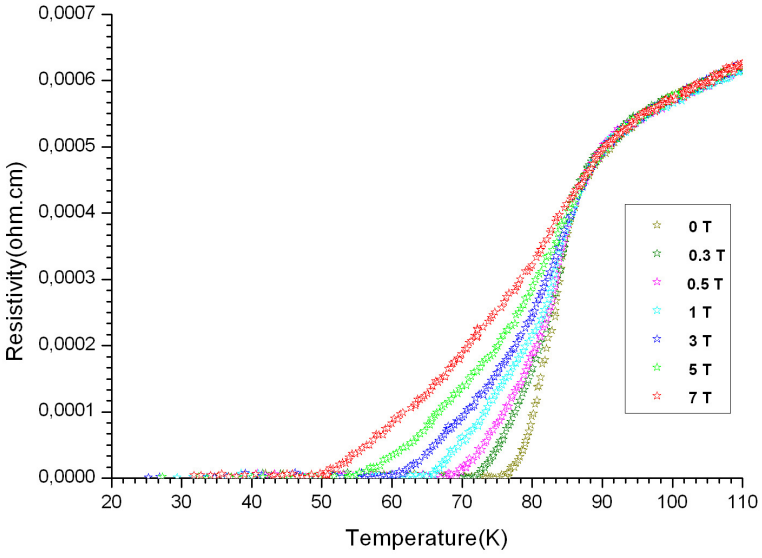

Figure 4.2: Resistivity versus temperature graph of $Bi_2Sr_2Ca_1Cu_2Ce_xO_y$ sample for x=0.001

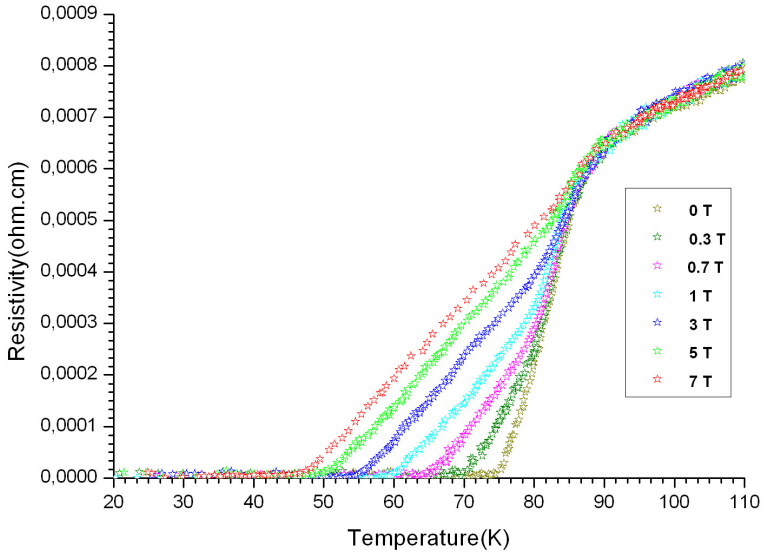

Figure 4.3: Resistivity versus temperature graph of $Bi_2Sr_2Ca_1Cu_2Ce_xO_y$ sample for x=0.003

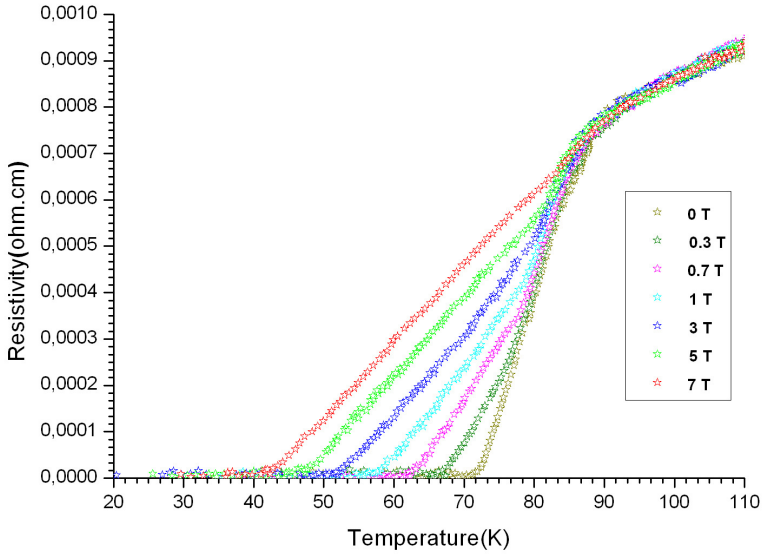

Figure 4.4: Resistivity versus temperature graph of $Bi_2Sr_2Ca_1Cu_2Ce_xO_y$ sample for x=0.005

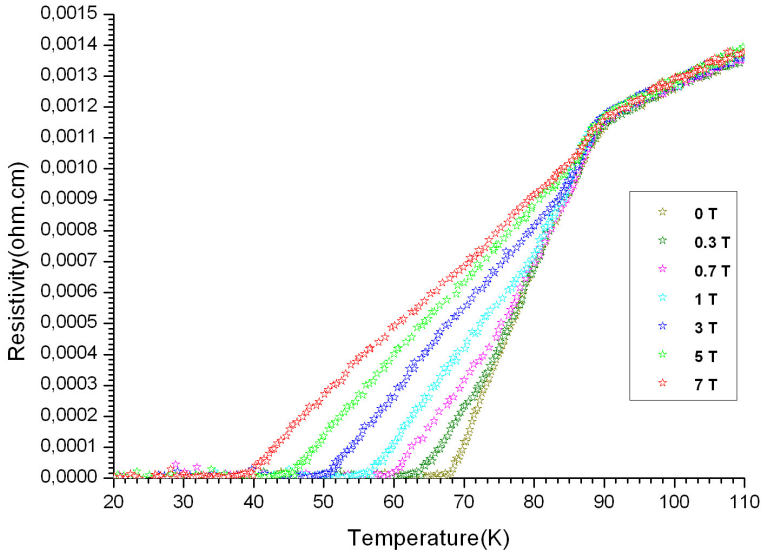

Figure 4.5: Resistivity versus temperature graph of $Bi_2Sr_2Ca_1Cu_2Ce_xO_y$ sample for x=0.01

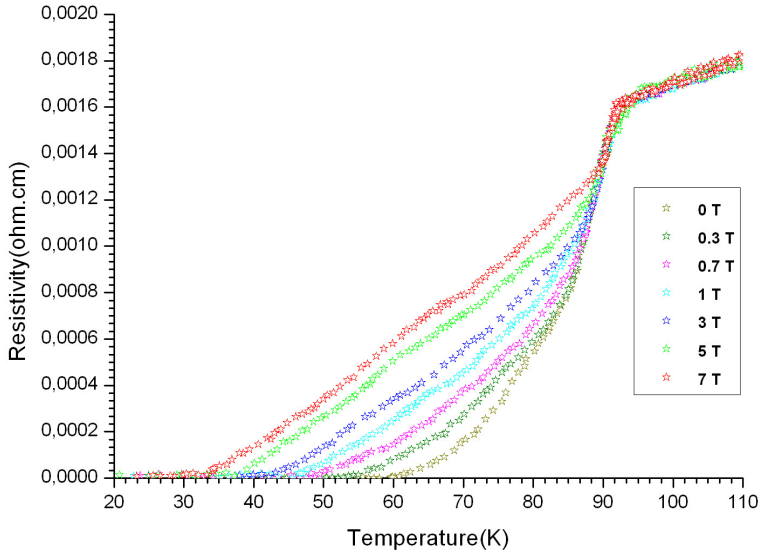

Figure 4.6: Resistivity versus temperature graph of $Bi_2Sr_2Ca_1Cu_2Ce_xO_y$ sample for x=0.03

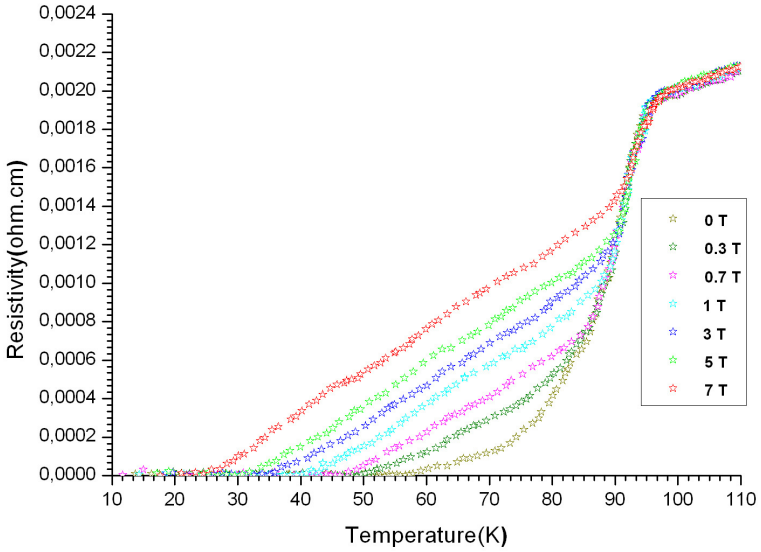

Figure 4.7: Resistivity versus temperature graph of $Bi_2Sr_2Ca_1Cu_2Ce_xO_y$ sample for x=0.05

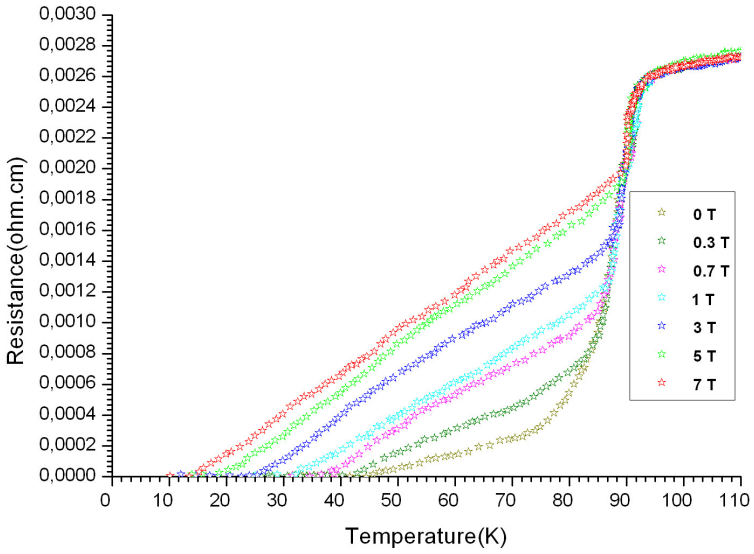

Figure 4.8: Resistivity versus temperature graph of $Bi_2Sr_2Ca_1Cu_2Ce_xO_y$ sample for x=0.1

As shown in figures, there is an increase of the critical onset temperature until 0.05 above. For x=0.1, the critical onset temperature decreases rapidly. The maximum T_c^{onset} was observed to be 95 K in x=0.05 whereas T_c^{onset} was noted to be as 89 K and 92 K in x=0 and x=0.1, respectively. However, the critical offset temperature decreases with increasing not only Ce concentration but also the magnitude of applied magnetic field. The T_c^{offset} of the pure (undoped) sample without applied magnetic field was noted to be 80 K, whereas for the (0.1 Ce-doped) sample, the T_c^{offset} was found to drop to 16 K with 7 T applied magnetic field. In addition, the width increases with increasing magnetic field for the same sample. Based on these results, this situation can be explained with the changes of hole concentration due to Ce addition. Ca^{2+} or Sr^{2+} ions in our system was said to replace Ce^{4+} ions. This is so because the ionic size of Ce^{4+} ion is in a good agreement with the ionic size of Ca^{2+} or Sr^{2+} ions. Moreover, Ce^{4+} ions replacing with Ca^{2+} or Sr^{2+} enables more electrons. That's why, this state attain the optimum hole concentration, and so the critical onset temperature increases with Ce concentration until above 0.05. Above this value, it is found that high concentration of Ce addition is too much for this structure. Hence, the structure worsened greatly, and the critical onset temperature decreases quickly. Furthermore, it is pointed out that all samples show metallic behaviour at high temperatures. Also, the resistivity at room temperature goes up with increasing in Ce addition, varying from (0.0030Ω.cm) for x = 0.1 to (0.0005 Ω.cm) for pure sample x = 0. It is thought that this can be sourced from the shrink of the grains, and so the contact points of grains increases. This leads to the increase in resistivity.

4.3 X-RAY DIFFRACTION(XRD) MEASUREMENTS

X-ray diffraction patterns for $Bi_2Sr_2Ca_1Cu_2Ce_xO_y$ samples were given in Figure 4.9– 4.16 below.

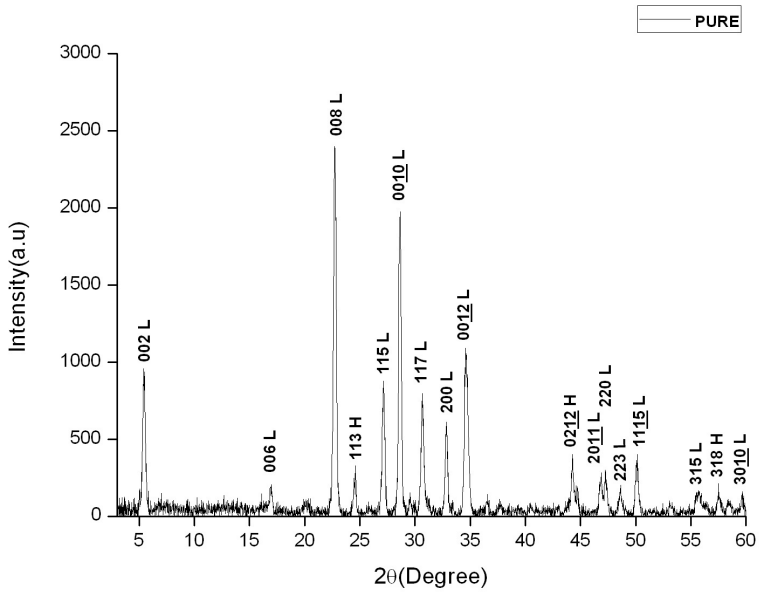

Figure 4.9: XRD patterns from the surface of $Bi_2Sr_2Ca_1Cu_2Ce_xO_y$ sample for x=0.0

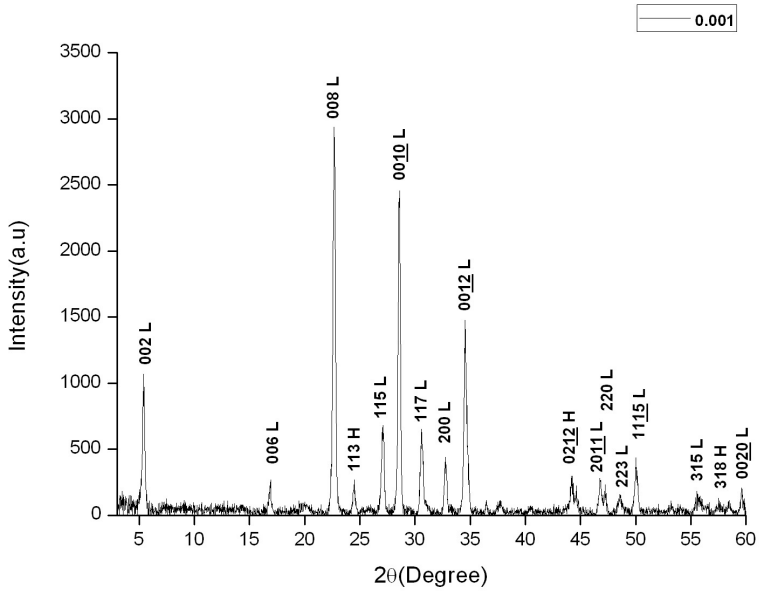

Figure 4.10: XRD patterns from the surface of $Bi_2Sr_2Ca_1Cu_2Ce_xO_y$ sample for x=0.001

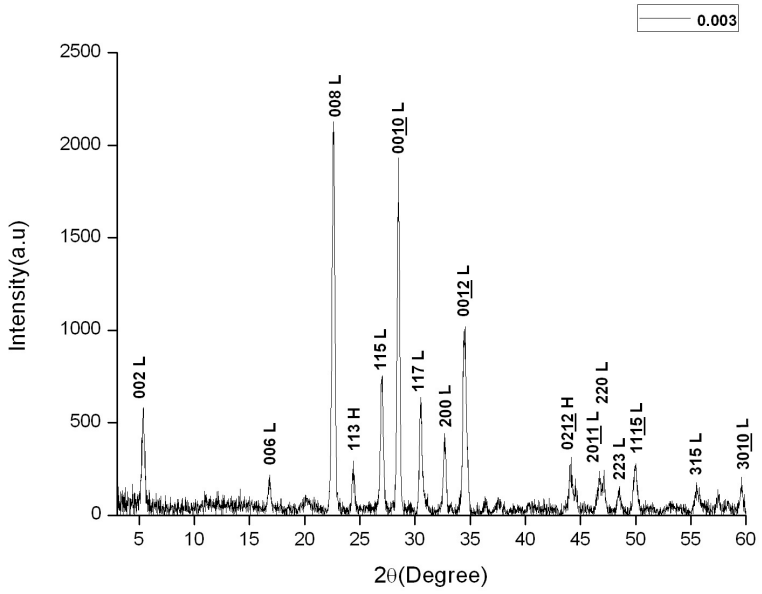

Figure 4.11: XRD patterns from the surface of $Bi_2Sr_2Ca_1Cu_2Ce_xO_y$ sample for x=0.003

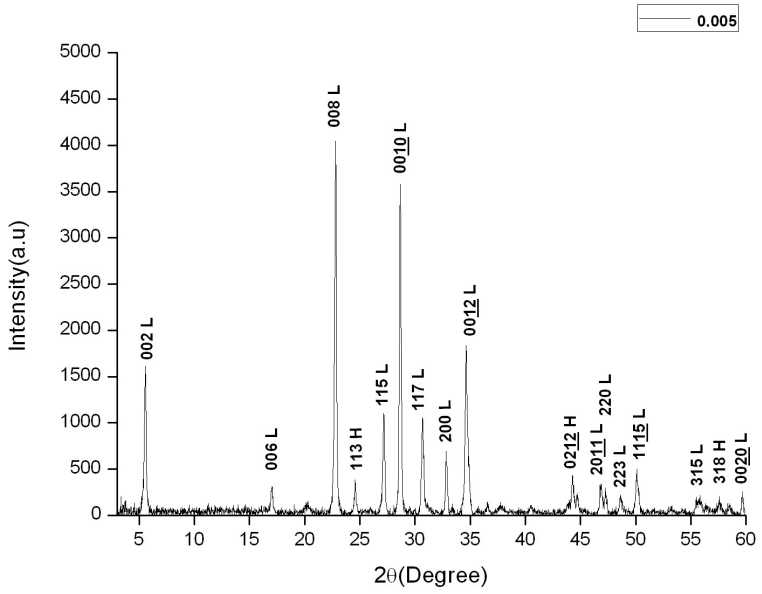

Figure 4.12: XRD patterns from the surface of $Bi_2Sr_2Ca_1Cu_2Ce_xO_y$ sample for x=0.005

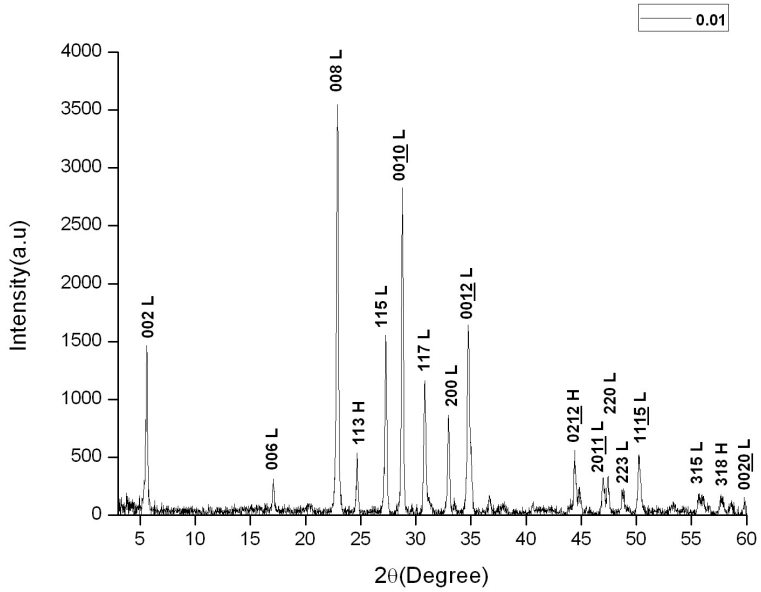

Figure 4.13: XRD patterns from the surface of $Bi_2Sr_2Ca_1Cu_2Ce_xO_y$ sample for x=0.01

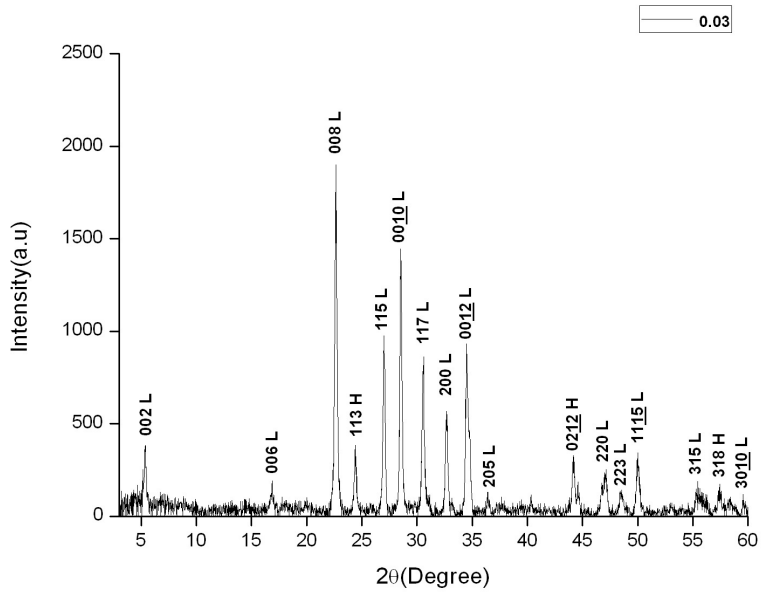

Figure 4.14: XRD patterns from the surface of $Bi_2Sr_2Ca_1Cu_2Ce_xO_y$ sample for x=0.03

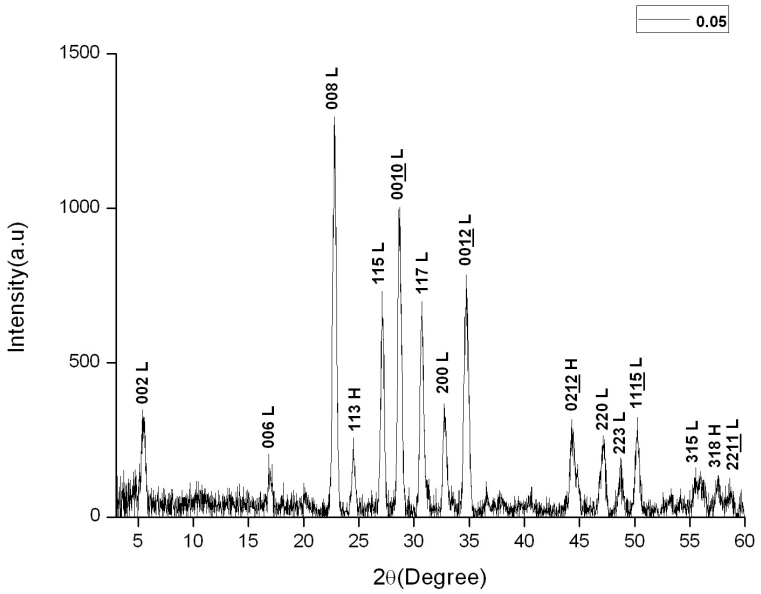

Figure 4.15: XRD patterns from the surface of $Bi_2Sr_2Ca_1Cu_2Ce_xO_y$ sample for x=0.05

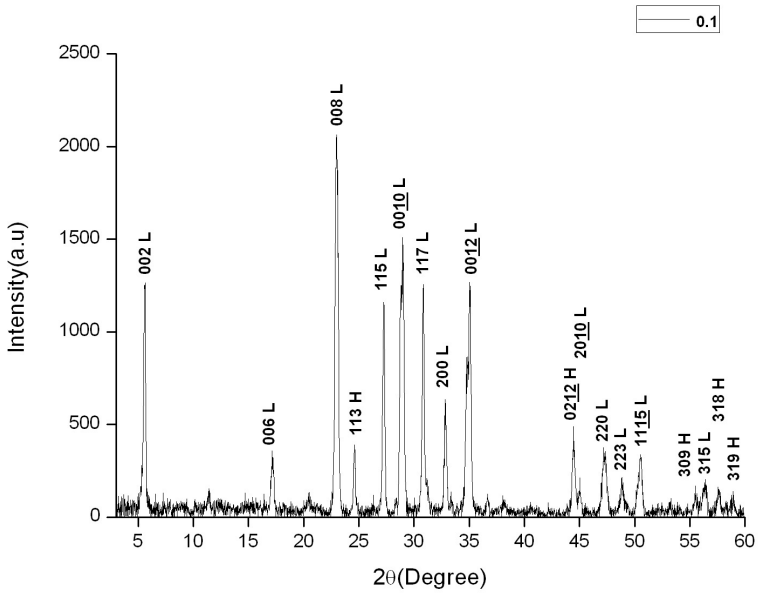

Figure 4.16: XRD patterns from the surface of $Bi_2Sr_2Ca_1Cu_2Ce_xO_y$ sample for x=0.1

(hkl) Miller indices and phases were shown on these graphs. (hkl) Miller indices were calculated by using the Equation

$$d^2 = \frac{1}{\frac{h^2}{a^2} + \frac{k^2}{b^2} + \frac{l^2}{c^2}} \tag{2.17}$$

Here, h,k,l are Miller indices and a,b,c are lattices parameters determined before for Bi-2212 and Bi-2223 phases. Besides, volume fractions of the Bi–2223 and Bi–2212 phases were calculated from the peak intensities of the same particular peaks by using the following Equations 2.18 and 2.19 **[55,56];**

$$f_{(2223)} = \frac{\sum I_{H(hkl)}}{\sum I_{H(hkl)} + \sum I_{L(hkl)}} \tag{2.18}$$

$$f_{(2212)} = \frac{\sum I_{L(hkl)}}{\sum I_{H(hkl)} + \sum I_{L(hkl)}} \tag{2.19}$$

(hkl)H and (hkl)L are the intensities of the (hkl) diffraction lines for Bi–2223 and Bi–2212 phases, respectively. Volume fractions and lattices parameters of the samples are listed in Table 4.2.

Samples	Lattice Parameter a (Å)	Lattice Parameter c (Å)	Volume Fractions (%)	
			2212	2223
x=0.0	5.40	31.51	94.97	5.03
x=0.001	5.41	31.41	94.58	5.42
x=0.003	5.43	31.02	94.39	5.61
x=0.005	5.44	30.81	94.33	5.67
x=0.01	5.46	30.54	93.07	6.93
x=0.03	5.47	30.31	91.45	8.55
x=0.05	5.48	30.16	91.22	8.78
x=0.1	5.49	30.09	92.18	7.82

Table 4.1: Lattice parameters a,c and volume fractions of $Bi_2Sr_2Ca_1Cu_2Ce_xO_y$ samples for x=0.0, 0.001, 0.003, 0.005, 0.01, 0.03, 0.05, 0.1.

From volume fraction results, it was found that Bi–2212 and Bi–2223 phases were observed in diffraction patterns of all samples for which, Bi–2212 phase is found to be dominant from Bi–2223 phase. Furthermore, it was pointed out that whereas the volume fraction of Bi–2212 phase decreases that of Bi–2223 phase increases until above x=0.05 which the volume fraction of Bi–2223 phase starts to decrease. Also, we know that if volume fraction of Bi–2223 phase increases, T_c^{onset} increases. Above x=0.05, T_c^{onset} value decreases because of the fact that volume fraction of Bi–2223 phase decreases. This result is consistent with the resistivity-temperature graphs. Based on lattice parameters results, it is clearly found that although lattice parameter *a* continuously increases with increasing Ce addition, parameter *c* decreases. This phenomenon can be explained that the Ce^{4+} ions might be replaced by either Ca^{2+} or Sr^{2+} ions. Namely; this replacement leads to form excess oxygen. This excess oxygen can be captured by BiO planes because of

oxygen deficiency, and so the positive charges decreases in plane. In addition, the bonding between planes becomes getting stronger. Therefore, this leads to decrease in the bond length of BiO planes and the length of lattice parameter c in structure. Conversely, we can say that there was a continuously increase in lattice parameter a with increasing in Ce addition. It is thought that this can be sourced from the increase in excess electrons and decrease in the effective valance of Cu. As a result, this situation brings about decreasing in the bond length of CuO planes and the length of lattice parameter a in structure, respectively.

4.4 SCANNING ELECTRON MICROSCOPY(SEM) MEASUREMENTS

The surface morphology of $Bi_2Sr_2Ca_1Cu_2Ce_xO_y$ samples were investigated by Scanning Electron Microscopy(SEM). SEM micrographs for all samples were shown in Figure 4.17-4.24.

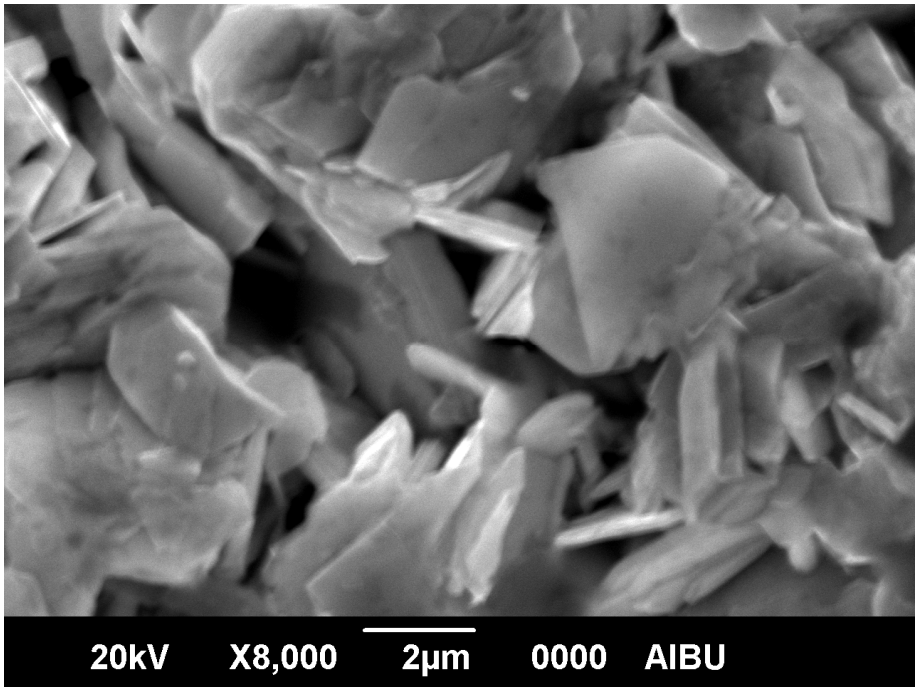

Figure 4.17: SEM micrographs of $Bi_2Sr_2Ca_2Cu_1Ce_xO_y$ sample for x=0.0

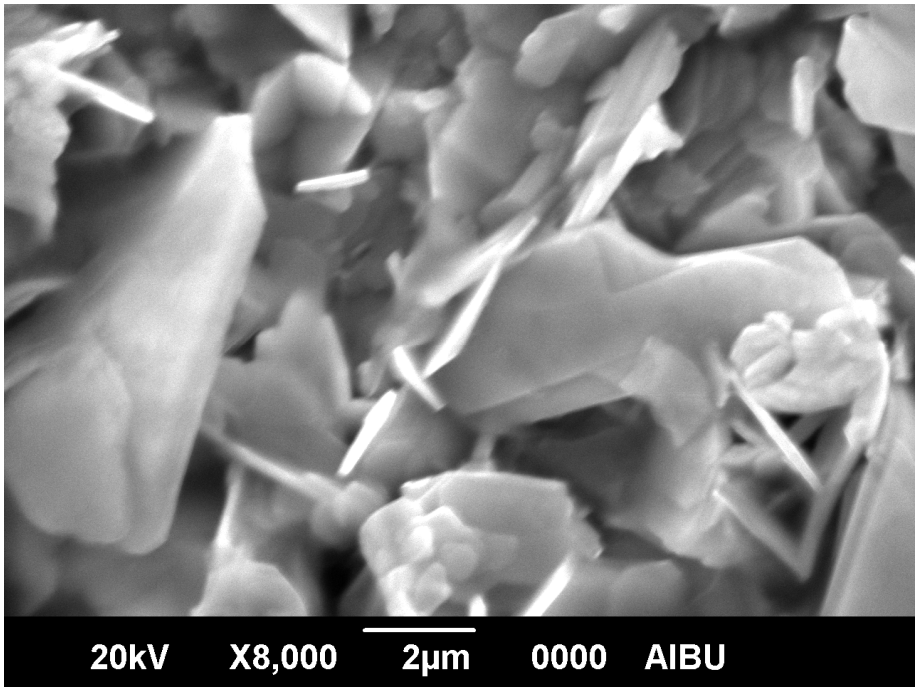

Figure 4.18: SEM micrographs of $Bi_2Sr_2Ca_2Cu_1Ce_xO_y$ sample for x=0.001

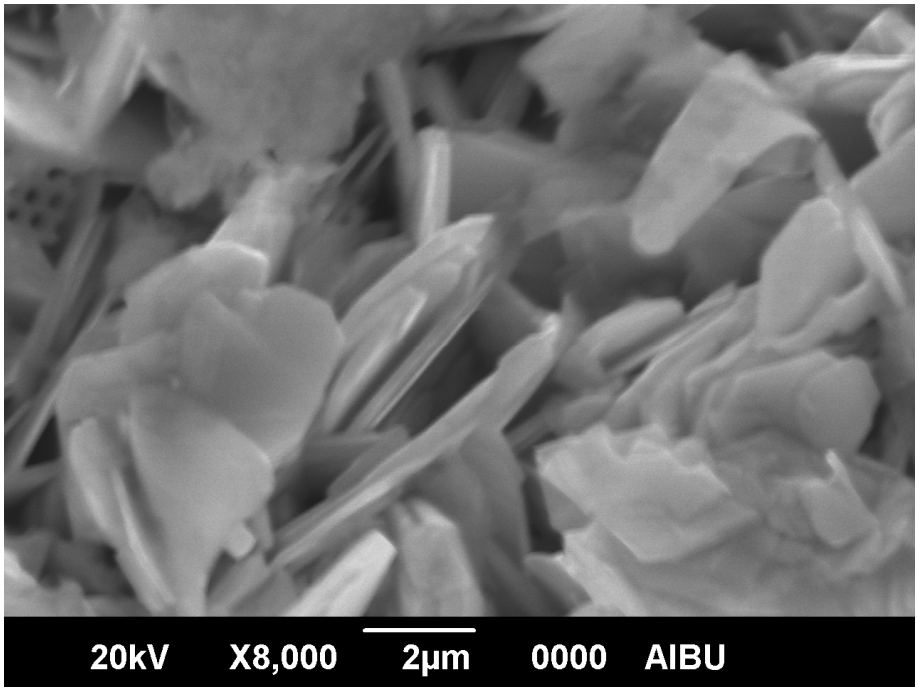

Figure 4.19: SEM micrographs of $Bi_2Sr_2Ca_2Cu_1Ce_xO_y$ sample for x=0.003

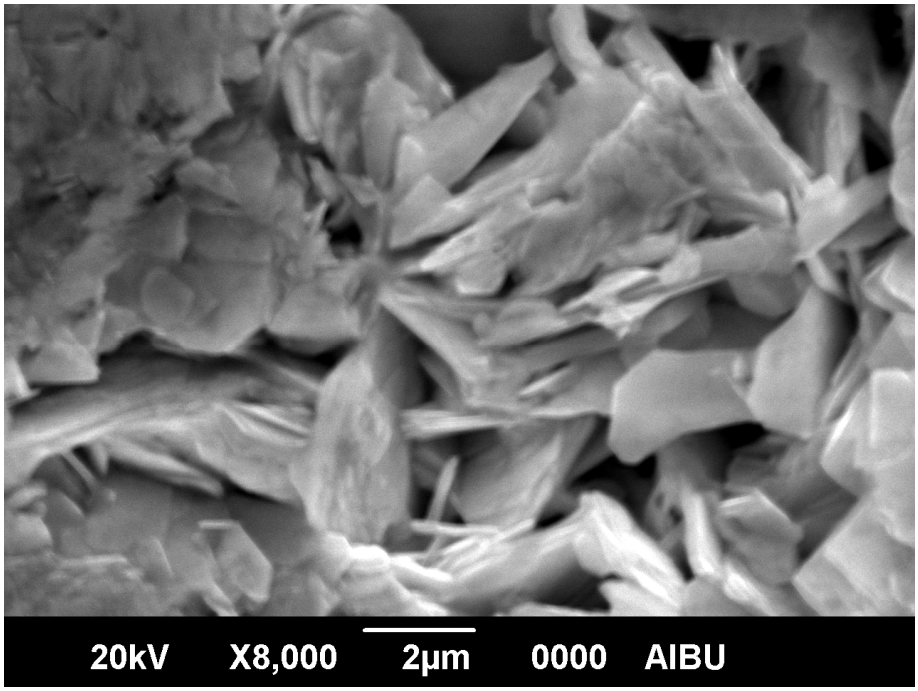

Figure 4.20: SEM micrographs of $Bi_2Sr_2Ca_2Cu_1Ce_xO_y$ sample for x=0.005

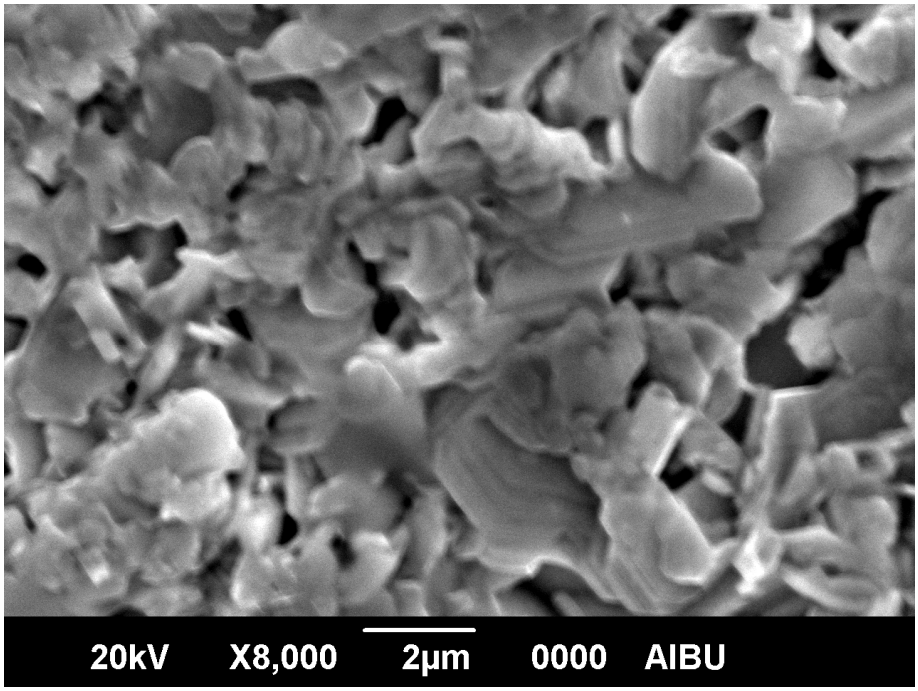

Figure 4.21: SEM micrographs of $Bi_2Sr_2Ca_2Cu_1Ce_xO_y$ sample for x=0.01

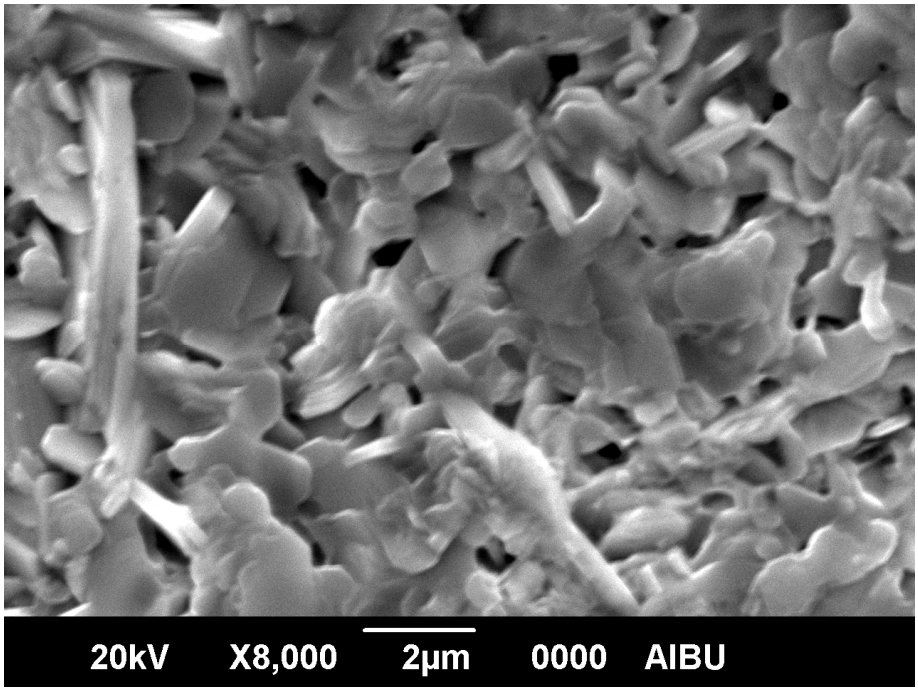

Figure 4.22: SEM micrographs of $Bi_2Sr_2Ca_2Cu_1Ce_xO_y$ sample for x=0.03

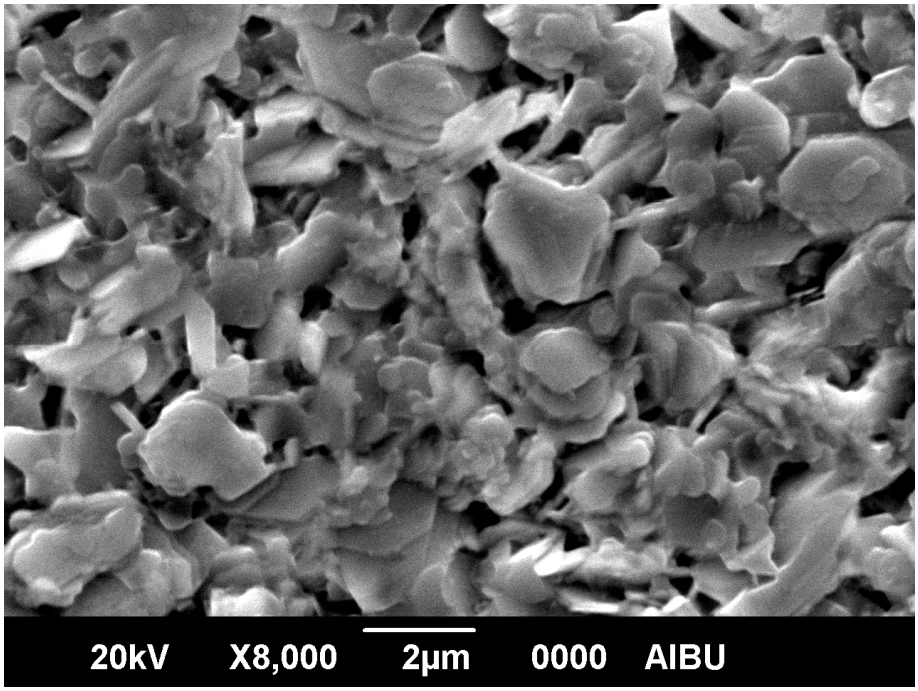

Figure 4.23: SEM micrographs of $Bi_2Sr_2Ca_2Cu_1Ce_xO_y$ sample for x=0.05

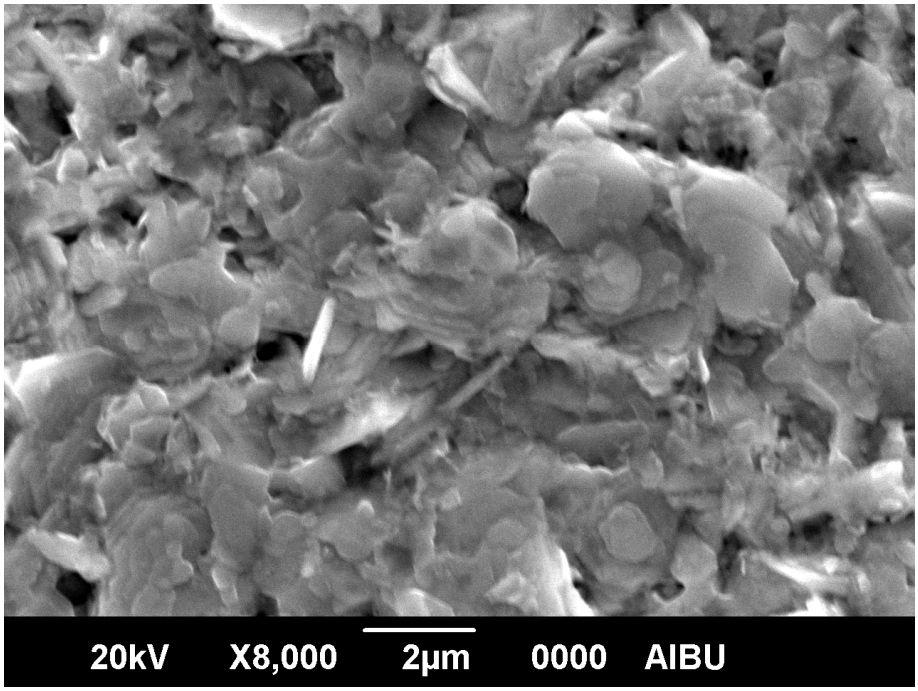

Figure 4.24: SEM micrographs of $Bi_2Sr_2Ca_2Cu_1Ce_xO_y$ sample for x=0.1

The micrographs in figures show that both the grains size and the grain connectivity were observed to decrease with increasing Ce addition. In addition, grain sizes were obtained to be in the range of between 408 and 540 nm for x=0.1 and x=0.0 samples by using image process. Besides, the broad grain size distribution can easily be seen from SEM micrographs of pure sample. Also, pure sample represents the uniform grain distribution and best crystallinity. However, it is obviously found that the sample doped with x=0.1 was noted to have the worst appearance among all samples. Based on these results of SEM investigations, surface morphology and grain connectivity of the samples were obtained to degrade with increase in the Ce addition. So, these results are in a good agreement with the resistivity measurements.

CHAPTER 5

CONCLUSION

In this study, we have investigated the effect of addition of Cerium in $Bi_2Sr_2Ca_1Cu_2Ce_xO_y$ superconductor with x=0, 0.001, 0.003, 0.005, 0.01, 0.03, 0.05 and 0.1 by means of resistivity measurements, XRD patterns, surface morphology. Based on the resistivity results, the critical onset temperature (T_c^{onset}) was found to increase with increase in Ce addition up to 0.05 above which the onset point of the sample rapidly started to decrease. The highest T_c^{onset} value was obtained at 95 K for x=0.05. It is clearly observed that volume fractions were in a good agreement with resistivity measurements. The reason of this result can be interpreted that the critical onset temperature (T_c^{onset}) of sample increases with the increase the volume fraction of Bi–2223 phase. In addition, it is found that the highest Bi–2223 volume fraction was obtained for x=0.05. Moreover, surface morphology, grain connectivity and phase ratio of the samples were obtained to degrade with increase in the Ce addition from SEM investigations. Based on these results, Ce addition was found to supress the superconducting properties.

REFERENCES

[1] G. Vidali, Superconductivity: The Next Revolution, Cambridge University Press, (1993).

[2] H.K. Onnes, Superconductivity and Magnetism. Comm. Phys. Lab. Univ. Leiden, (1911), 119–120.

[3] W. Meissner, R. Ochsenfeld, Naturwiss., 21, (1933), 787-788.

[4] S.A. Zhou, Electrodynamics of Solids and Microwave Superconductivity JohnWiley&Sons, Inc., (1999).

[5] Y.M. Galperin, Introduction to Modern Solid State Physics, (2001).

[6] V.L. Ginzburg, L.D. Landau, J.Exptl. Theoret. Phys. (U.S.S.R), 20, 1064 (1950).

[7] J. Bardeen, L. N. Cooper, J. R. Schrieffer, Theory of Superconductivity, Phys. Rev., 108**,** (1957), 1175–1205.

[8] A.A. Abrikosov, Zh. Eksp. Teor. Fiz., 32, 1442 (1957).

[9] B.D. Josephson, Phys. Lett.**,** 1, 251 (1962).

[10] J.G. Bednorz, K.A. Muller, Possible High T_c Superconductivity in the Ba-La-Cu-O System, Z.Phys., 64 (1986), 189-193.

[11] C. Mitchell, M. Hervieu, M.M. Borel, A. Grandin, F. Deslandes, J. Provost, B. Raveau, Superconductivity in Bi-Sr-Ca-Cu-O System, Z. Phys. B. Condensed Matter 68, (1987), 421-423.

[12] M.K. Wu, J.R. Ashburn, C. Torng, Superconductivity at 93 K in a New Mixed-Phase Y-B-Cu-O Compound System at Ambient Pressure, Phys. Rev. Lett. 58, 9 (1987), 908–910.

[13] H. Maeda, Y. Taraka, Measurement of the Normal State Anisotropic Resistivity of Single Crystal Bi-Sr-Ca-Cu-O, Jpn.Appl.Phys., 27, 2 (1988), L209-L211.

[14] M.R. Hazen, L.W. Finger, R.J. Angel, T.C. Prewith, R.L. Ross, A.M. Hermann, A New High-T_c Oxide Superconductor Without a Rare-Earth Element, Phys. Rev. Lett**.,** 60, 657 (1998).

[15] A. Schilling, M. Cantoni, J.D. Guo, H.R. Ott, Superconductivity Above 130-K in the Hg-Ba-Ca-Cu-O System, Nature, 363, 6424 (1993), 56–58.

[16] L. Gao, Z.J. Huang, R.L. Meng, J.G. Lin, F. Chen, L. Beauvais, Y.Y. Sun, Y.Y. Xue, C.W. Chu, Study of Superconductivity in the Hg-Ba-Ca-Cu-O System, Physica C**,** 213, 3–4 (1993), 261–265.

[17] J. Nagamatsu, N. Nakagawa, T. Muranaka, Y. Zenitani, J. Akimitsu, Superconductivity at 39 K in Magnesium Diboride, Nature, 410, 6824 (2001), 63–64.

[18] M.A. Omar, Elementary Solid State Physics. Addison-Wesley Publishing Company, (1993).

[19] A.C. Rose-Innes, E.H. Rhoderic, Introduction to Superconductivity, Butterworth –Heineman, (1978).

[20] M. Cyrot, D. Pavuna, Introduction to Superconductivity and High T_c Materials, (1992).

[21] R.A. Serway, Physics for Scientists and Engineers, Thomson Brooks/Cole, (1992).

[22] A.B. Pippard, An Experimental and Theoretical Study of the Relation Between Magnetic Field and Current in Superconductor, Proc. Roy. Soc. A, 216, (1953), 547–568.

[23] J.R. Hook, H.E. Hall, Solid State Phiysics, John Wiley & Sons Ltd., (1991).

[24] C. Kittel, Introduction to Solid State Physics. John Wiley & Sons, Inc., (1986).

[25] A.S. Alexandrow, High Temparature Superconductors and Other Superfluids, Taylor Francis, (1994).

[26] J.C. Phillips, Physics of High T_c Superconductors, Academic Press, (1989).

[27] P.P. Charles, Jr.T. Datta, H.A. Farach, Copper Oxide Superconductors, Wiley-Interscience, (1988).

[28] H. Ateş, Master Thesis, Inönü University, (1998).

[29] T.P. Sheahen, Introduction to High Temperature Superconductivity, Kluwer Academic Publishers, (2002).

[30] T.D. Dzhafarov, Diffusion in High-Temperature Superconductors, Phys. Status Solidi A, 158, 2 (1996), 335–358.

[31] M. Murakami, Processing of Bulk YBCO, Supercond. Sci. Technol., 5, 4 (1992), 185-203.

[32] I.M. Chapnik, Superconductivity and the Periodic Table, J. Of Matt. Science Lett., 4, 3 (1985), 370-372.

[33] J.R. Gavalev, Appl. Phys. Lett., 23, (1973), 480.

[34] L.R. Testardi, J.H. Werniek, W.A. Roger, Salid State Commun., 15, (1974), 1.

[35] R.J. Cava, R.B. Van Dover, B. Battlog, E.A. Rietman, Bulk Superconductivity at 36 K in $La_{1.8}Sr_{0.2}CuO_4$, Phys. Rev. Lett., 58, 4 (1987), 408-410.

[36] P.M. Grant, M.B. Beyers, E.M. Engler, G. Lim, S.S.P. Parkin, M.L. Ramirez, V.Y. Lee, A. Nazzal, J.E. Vazquez, R.J. Sovay, Superconductivity Above 90 K in the Compound $YBa_2Cu_3O_{7-x}$, Phys. Rev. B, 35, 13 (1987), 7242–7244.

[37] S.B. Quadri, L.E. Toth, M. Osofsky, S. Lawrence, D.U. Gubser, S.A. Wolf, X-Ray Identification of Supercunducting High T_c Phase in Y-Ba-Cu-O System, Phys. Rev. B, 35, 13 (1987), 7235–7237.

[38] S.J. Hwu, S.N. Song, J. Thiel, K.R. Poeppelmeier, J.B. Ketterson, A.J. Freeman, High T_c Superconductivity in Regions of Possible Compound Formation, Phys. Rev. B, 35, 13 (1987), 7119–7121.

[39] J.M. Tarascon, L.H. Green, W.R. McKinnon, G.W. Hull, Superconductivity at 90 K in Multiphase of Y-Ba-Cu-O, Phys. Rev. B, 35, 13 (1987), 7115–7117.

[40] K. Tokano, Properties of Pb-Doped Bi-Sr-Ca-Cu-O Superconductors, Appl. Phys. Lett., 53, 14 (1988), 1329-1331.

[41] A.A. Qidwai, M. Humayun, S.M. Ziaulhaque, D.Ahmad, A. Saghır, Preparation and High-T_c Measurements of the $Bi_{1.6}Pb_xSb_ySr_2Ca_2Cu_3O_\delta$ Superconducting Systems with x=0.4,0.3,0.1 and y=0,0.1,0.3, Supercond.Sci.Technol., 5, 10 (1992), 602-604.

[42]S.S.P. Parkin, V.Y. Lee, A.I. Nazzal, R. Savoy, T.C. Huang, G. Gorman, R. Beyers, Model Family of High-Temperature Superconductors -$Tl_mCa_{n-1}Ba_2Cu_nO_{2(n+1)+m}$ (m=1,2 - n=1,2,3), Phys. Rev. B, 38, 10 (1988), 6531–6537.

[43] Z.Z. Sheng, A.M. Hermann, Bulk Superconductivity at 120-K in the Tl-Ca-Ba-Cu-O System, Nature, 332, 6160 (1988), 138–139.

[44] J.B. Torrance, Y. Tokura, S. Laplaca, T.C. Huang, R.J. Savoy, A.I. Nazzal, New Class of High - T_c Structures - Intergrowth of Multiple Copper – Oxide Perovskite Like Layers with Double Sheets of Bio, Solid State Commun., 66, 7 (1988), 703-706.

[45] O. Oztürk, Ph-D Thesis, Abant Izzet Baysal University, (2007).

[46] M.J. Tarascon, Y. Le Page, Phys. Rev. B 37, (1988).

[47] Y. Mei, S.M. Green, C. Jiang, H.L. Luo, Phase Formation in a Bi-Sr-Ca-Cu Oxide Superconductor, J. Appl. Phys., 64, 12 (1988), 6795-6799.

[48] A. Kiliç, Master Thesis, University of Ankara, (2000).

[49] R.P. Gupta, M. Gupta, Electronic Structure Investigation of the Relationship Between Oxygen Ordering and Superconductivity in $YBa_2Cu_3O_{6.5}$, Physica C, 171, 5 (1990), 465–467.

[50] W. Zhu, P.S. Nicholson, The Quantitative X-Ray Phase Analysis in Bi-(Pb)-Sr-Ca-Cu-O Superconductor System, Matt. Lett., 12, 3 (1991), 191-194.

[51] M.A. Subramanian, C.C. Torardi, J. Gopalakrishnan, J.C. Calabrese, K.J. Morrissey, T.R. Askew, R.B. Flippen, U. Chowdhry, A.W. Sleight, J.J. Lin, S.J. Poon New Oxide Superconductors, Physica C, 153, Part 1 (1988), 608–612.

[52] Z.Z. Sheng, A.M. Hermann, Bulk Superconductivity at 120 K in the Tl–Ca/Ba–Cu–O System, Nature, 332, (1988), 55–58.

[53] S.N. Putilin, E.V. Antipov, O. Chmaissem, M. Manezio, Superconductıvıty at 94-K in $HgBa_2CuO_{4+\delta}$, Nature, 362, 6417 (1993), 226–228.

[54] E.M. Engler, Superconductivity at Accessible Temperatures, Chemtech., 17, 9 (1987), 542-551.

[55] C.W. Chu, R.L. Meng, L. Gao, Z.J. Huang, F. Chen, Y.Y. Xue, Superconductivity Above 150-K in $HgBa_2Ca_2Cu_3O_{8+\delta}$ at High-Pressures, Nature, 365, 6444 (1993), 323–325.

[56] S.A. Halim, S.A. Khawaldeh, S.B. Mohammed, H. Azhan, Superconducting Properties of $Bi_{2-x}Pb_xSr_2Ca_2Cu_3O_y$ System Derived via Sol-Gel and Solid State Routes, Mater. Chem. Phys., 61, 3 (1999), 251-259.